

1 **Reply to the Editor**

2 Dear Editor,

3 Thank you very much for your comments. We cited some more recent papers, e.g. Sprenger et
4 al. (2016a, b), Stumpp and Hendry (2012), Geris et al. (2015), Peralta-Tapia et al. (2015),
5 Bertrand et al. (2014), Wang et al. (2010), and Muñoz-Villers and McDonnell (2012) and
6 updated our reference list, accordingly. Furthermore, we added the $\delta^2\text{H}$ and $\delta^{18}\text{O}$ time series of
7 GNIP station Koblenz to Figure 2. We followed your suggestion and edited the colour coding
8 of Figure 10.

9 All changes we made to the manuscript can be found below.

10 We are hoping that our manuscript is ready for publication now.

11

12 On behalf of the authors,

13 Natalie Orłowski

14 **Exploring water cycle dynamics by sampling multiple**
15 **stable water isotope pools in a developed landscape of**
16 **Germany**

17

18 **N. Orlowski^{1,2}, P. Kraft¹, J. Pferdmenges¹ and L. Breuer^{1,3}**

19 [1]{Institute for Landscape Ecology and Resources Management (ILR), Research Centre for
20 BioSystems, Land Use and Nutrition (iFZ), Justus Liebig University Giessen, Giessen,
21 Germany}

22 [2]{Global Institute for Water Security, University of Saskatchewan, Saskatoon, Canada}

23 [3]{Centre for International Development and Environmental Research, Justus Liebig
24 University Giessen, Germany}

25 Correspondence to: N. Orlowski (Natalie.Orlowski@umwelt.uni-giessen.de)

26

27 **Abstract**

28 A dual stable water isotope ($\delta^2\text{H}$ and $\delta^{18}\text{O}$) study was conducted in the developed (managed)
29 landscape of the Schwingbach catchment (Germany). The two-year weekly to biweekly
30 measurements of precipitation, stream, and groundwater isotopes revealed that surface and
31 groundwater are isotopically disconnected from the annual precipitation cycle but showed
32 bidirectional interactions between each other. Apparently, snowmelt played a fundamental role
33 for groundwater recharge explaining the observed differences to precipitation δ -values.

34 A spatially distributed snapshot sampling of soil water isotopes in two soil depths at 52
35 sampling points across different land uses (arable land, forest, and grassland) revealed that top
36 soil isotopic signatures were similar to the precipitation input signal. Preferential water flow
37 paths occurred under forested soils explaining the isotopic similarities between top and subsoil
38 isotopic signatures. Due to human-impacted agricultural land use (tilling and compression) of
39 arable and grassland soils, water delivery to the deeper soil layers was reduced, resulting in
40 significant different isotopic signatures. However, the land use influence became less
41 pronounced with depth and soil water approached groundwater δ -values. Seasonally tracing
42 stable water isotopes through soil profiles showed that the influence of new percolating soil

43 water decreased with depth as no remarkable seasonality in soil isotopic signatures was obvious
44 at depth >0.9 m and constant values were observed through space and time. Since classic
45 isotope evaluation methods such as transfer function based mean transit time calculations did
46 not provide a good fit between the observed and calculated data, we established a hydrological
47 model to estimate spatially distributed groundwater ages and flow directions within the
48 Vollnkirchener Bach subcatchment. Our model revealed that complex age dynamics exist
49 within the subcatchment and that much of the runoff must have been stored for much longer than
50 event water (average water age is 16 years). Tracing stable water isotopes through the water
51 cycle in combination with our hydrological model was valuable for determining interactions
52 between different water cycle components and unravelling age dynamics within the study area.
53 This knowledge can further improve catchment specific process understanding of developed,
54 human-impacted landscapes.

55 **1 Introduction**

56 The application of stable water isotopes as natural tracers in combination with hydrodynamic
57 methods has been proven to be a valuable tool for studying the origin and formation of
58 recharged water as well as the interrelationship between surface water and groundwater
59 (Blasch and Bryson, 2007), partitioning evaporation and transpiration (Wang and Yakir,
60 2000), and mixing processes between various water sources (Clark and Fritz, 1997c).
61 Particularly in catchment hydrology, stable water isotopes play a major role since they can be
62 utilised for hydrograph separations (Buttle, 2006), to calculate the mean transit time (McGuire
63 and McDonnell, 2006), to investigate water flow paths (Barthold et al., 2011), or to improve
64 hydrological model simulations (Windhorst et al., 2014). However, most of our current
65 understanding is resulting from studies in forested catchments. Spatio-temporal studies of
66 stream water in developed, agricultural dominated, and managed catchments are less
67 abundant. This is partly caused by damped stream water isotopic signatures excluding
68 traditional hydrograph separations in low-relief catchments (Klaus et al., 2015). Unlike the
69 distinct watershed components found in steeper headwater counterparts, lowland areas often
70 exhibit a complex groundwater–surface water interaction (Klaus et al., 2015). Sklash and
71 Farvolden (1979) showed that groundwater plays an important role as a generating factor for
72 storm and snowmelt runoff processes. In many catchments, streamflow responds promptly to
73 rainfall inputs but variations in passive tracers such as water isotopes are often strongly
74 damped (Kirchner, 2003). This indicates that storm runoff in these catchments is dominated
75 mostly by “old water” (Buttle, 1994; Neal and Rosier, 1990; Sklash, 1990). However, not all

76 “old water” is the same (Kirchner, 2003). This catchment behaviour was described by
77 Kirchner (2003) as the old water paradox. Thus, there is evidence of complex age dynamics
78 within catchments and much of the runoff is stored in the catchment for much longer than
79 event water (Rinaldo et al., 2015). Still, some of the physical processes controlling the release
80 of “old water” from catchments are poorly understood, roughly modelled, and the observed
81 data do not suggest a common catchment behaviour (Botter et al., 2010). However, old water
82 paradox behaviour was observed in many catchments worldwide but it may have the strongest
83 effect in agriculturally managed catchments, where surprisingly only small changes in stream
84 chemistry have been observed (Hrachowitz et al., 2016).

85 Moreover, almost all European river systems were already substantially modified by humans
86 before river ecology research developed (Allan, 2004). Through changes in land use, land
87 cover, irrigation, and draining, agriculture has substantially modified the water cycle in terms
88 of both quality and quantity (Gordon et al., 2010) as well as hydrological functioning (Pierce et
89 al., 2012). Hrachowitz et al. (2016) recently stated the need for a stronger linkage between
90 catchment-scale hydrological and water quality communities. Further, McDonnell et al. (2007)
91 concluded that we need to figure out a way to embed landscape heterogeneity or the
92 consequence of the heterogeneity (i.e. of agricultural dominated and managed catchments) into
93 models as current generation catchment-scale hydrological and water quality models are poorly
94 linked (Hrachowitz et al., 2016).

95 One way to better understand catchment behaviour and the interaction among the various water
96 sources (surface, subsurface, and groundwater) and their variation in space and time is a detailed
97 knowledge about their isotopic composition. In principal, isotopic signatures of precipitation
98 are altered by temperature, amount (or rainout), continental, altitudinal, and seasonal effects.
99 Stream water isotopic signatures can reflect precipitation isotopic composition and moreover,
100 dependent on discharge variations be affected by seasonally variable contributions of different
101 water sources such as bidirectional water exchange with the groundwater body during baseflow,
102 or high event-water contributions during stormflow (Genereux and Hooper, 1998; Koeniger et
103 al., 2009). Precipitation falling on vegetated areas is partly intercepted by plants and re-
104 evaporated isotopically fractionated. The remaining throughfall infiltrates slower and can be
105 affected by evaporation resulting in an enrichment of heavy isotopes, particularly in the upper
106 soil layers (Gonfiantini et al., 1998; Kendall and Caldwell, 1998). In the soil, specific isotopic
107 profiles develop, characterized by an evaporative layer near the surface. The isotopic

108 enrichment decreases exponentially with depth, representing a balance between the upward
109 convective flux and the downward diffusion of the evaporative signature (Barnes and Allison,
110 1988). In humid and semi-humid areas, this exponential decrease is generally interrupted by the
111 precipitation isotopic signal. Hence, the combination of the evaporation effect and the
112 precipitation isotopic signature determine the isotope profile in the soil (Song et al., 2011).
113 Once soil water reaches the saturated zone, this isotope information is finally transferred to the
114 groundwater (Song et al., 2011). Soil water can therefore be seen as a link between precipitation
115 and groundwater, and the dynamics of isotopic composition in soil water are indicative of the
116 processes of precipitation infiltration, evaporation of soil water, and recharge to groundwater
117 (Blasch and Bryson, 2007; Song et al., 2011).

118 We started our research with results obtained through an earlier study in the managed
119 Schwingbach catchment that implied a high responsiveness of the system to precipitation inputs
120 indicated by very fast rises in discharge and groundwater head levels (Orlowski et al., 2014).
121 However, as there was only a negligible influence of the precipitation input signal on the stable
122 water isotopic composition in streams, our initial data set showed evidence for complex age
123 dynamics within the catchment. Nevertheless, a rapid flow response to a precipitation input may
124 also be mistaken (as conceptualized in the vast majority of catchment-scale conceptual
125 hydrological models) as the actual input signal already reaching the stream, while in reality it
126 is the remainder of past input signals that slowly travelled through the system (Hrachowitz et
127 al., 2016). The observable hydrological response therefore acts at different time scales than the
128 tracer response (Hrachowitz et al., 2016) as described by the celerity vs. velocity concept
129 (McDonnell and Beven, 2014). The observed patterns in our catchment therefore inspired us to
130 use a combined approach of hydrodynamic data analyses, stable water isotope investigations,
131 and data-driven hydrological modelling to determine catchment dynamics (response times and
132 groundwater age patterns) and unravel water flow paths at multiple spatial scales. This work
133 should further improve our knowledge on hydrological flow paths in developed, human-
134 impacted catchments.

135 **2 Materials and methods**

136 **2.1 Study area**

137 The research was carried out in the Schwingbach catchment (50°30'4.23"N, 8°33'2.82"E)
138 (Germany) (Fig. 1a). The Schwingbach and its main tributary the Vollnkirchener Bach are low-

139 mountainous creeks having an altitudinal difference of 50–100 m over 5 km distance (Perry and
140 Taylor, 2009) (Fig. 1c) with an altered physical structure of the stream system (channelled
141 stream reaches, pipes, drainage systems, fishponds). The Schwingbach catchment (9.6 km²)
142 ranges from 233–415 m a.s.l. with an average slope of 8.0%. The Vollnkirchener Bach tributary
143 is 4.7 km in length and drains a 3.7 km² subcatchment area (Fig. 1c), with elevations from 235–
144 351 m a.s.l. Almost 46% of the overall Schwingbach catchment is forested, which slightly
145 exceeds agricultural land use (35%) (Fig. 1c). Grassland (10%) is mainly distributed along
146 streams and smaller meadow orchards are located around the villages.

147 The Schwingbach main catchment is underlain by argillaceous shale in the northern parts,
148 serving as aquicludes. Graywacke zones with lydite in the central, as well as limestone, quartzite,
149 and sandstone regions in the headwater area provide aquifers with large storage capacities (Fig.
150 1f). Loess covers Paleozoic bedrock at north- and east bounded hillsides (Fig. 1f). Streambeds
151 consists of sand and debris covered by loam and some larger rocks (Lauer et al., 2013). Many
152 downstream sections of both creeks are framed by armor stones (Orlowski et al., 2014). The
153 dominant soil types in the overall study area are Stagnosols (41%) and mostly forested
154 Cambisols (38%). Stagnic Luvisols with thick loess layers, Regosol, Luvisols, and Anthrosols
155 are found under agricultural use and Gleysols under grassland along the creeks.

156 [Figure 1 near here]

157 The climate is classified as temperate with a mean annual temperature of 8.2°C. An annual
158 precipitation sum of 633 mm (for the hydrological year 1 November 2012 to 31 October 2013)
159 was measured at the catchment's climate station (site 13, Fig. 1b). The year 2012 to 2013 was
160 an average hydrometeorological year. For comparison, the climate station Giessen/Wettenberg
161 (25 km N of the catchment) operated by the German Meteorological Service (DWD, 2014)
162 records a mean annual temperature of 9.6 °C and a mean annual precipitation sum of 666±103
163 mm for the period 1980–2010. Discharge peaks from December to April (measured by the use
164 of RBC-flumes with maximum peak flow of 114 L s⁻¹, Eijkelkamp Agrisearch Equipment,
165 Giesbeek, NL) and low flows occur from July until November. Substantial snowmelt peaks
166 were observed during December 2012 and February 2013. Furthermore, May 2013 was an
167 exceptional wet month characterised by discharge of 2–3 mm d⁻¹. A detailed description of
168 runoff characteristics is given by Orlowski et al. (2014).

169 **2.2 Monitoring network and water isotope sampling**

170 The monitoring network consists of an automated climate station (site 13, Fig. 1 b–c) (Campbell
171 Scientific Inc., AQ5, UK; equipped with a CR1000 data logger), three tipping buckets, and 15
172 precipitation collectors, six stream water sampling points, and 22 piezometers (Fig. 1 b–c).
173 Precipitation data were corrected according to Xia (2006).

174 Two stream water sampling points (sites 13 and 18) in the Vollnkirchener Bach are installed
175 with trapezium shaped RBC-flumes for gauging discharge (Eijkelkamp Agrisearch Equipment,
176 Giesbeek, NL), and a V-weir is located at sampling point 64. RBC-flumes and V-weir are
177 equipped with Mini-Divers® (Eigenbrodt Inc. & Co. KG, Königsmoor, DE) for automatically
178 recording water levels. Discharge at the remaining stream sampling points was manually
179 measured applying the salt dilution method (WTW-cond340i, WTW, Weilheim, DE). The 22
180 piezometers (Fig. 1b) are made from perforated PVC tubes sealed with bentonite at the upper
181 part of the tube to prevent contamination by surface water. For monitoring shallow groundwater
182 levels, either combined water level/temperature loggers (Odyssey Data Flow System,
183 Christchurch, NZ) or Mini-Diver® water level loggers (Eigenbrodt Inc. & Co. KG,
184 Königsmoor, DE) are installed. Accuracy of Mini-Diver® is ± 5 mm and for Odyssey data
185 logger ± 1 mm. For calibration purposes, groundwater levels are additionally measured
186 manually via an electric contact gauge.

187 Stable water isotope samples of rainfall, stream-, and groundwater were taken from July 2011
188 to July 2013 on weekly intervals. In winter 2012–2013, snow core samples over the entire snow
189 depth of <0.15 m were collected in tightly sealed jars at same sites as open rainfall was sampled.
190 We sampled shortly after snow fall because sublimation, recrystallization, partial melting,
191 rainfall on snow, and redistribution by wind can alter the isotopic composition (Clark and Fritz,
192 1997b). Samples were melted overnight following Kendall and Caldwell (1998) and analysed
193 for their isotopic composition. Open rainfall was collected in self-constructed samplers as per
194 Windhorst et al. (2013). Grab samples of stream water were taken at six locations, three
195 sampling points at each stream (Fig. 1b–c). Since spatial isotopic variations of groundwater
196 among piezometers under meadow were small, samples were collected at three out of eight
197 sampling points under meadow (sites 1, 6, and 21), five under the arable field (sites 25–29), and
198 four next to the Vollnkirchener Bach (sites 24, 31, 32, and 35) (Fig. 1b). Additionally, a
199 drainage pipe (site 15) located ~ 226 m downstream of site 18 was sampled. According to IAEA

200 standard procedures, all samples were filled and stored in 2 mL brown glass vials, sealed with
201 a solid lid, and wrapped up with Parafilm®.

202 **2.3 Isotopic soil sampling**

203 **2.3.1 Spatial variability**

204 In order to analyse the effect of small-scale characteristics such as distance to stream, TWI, and
205 land use on soil isotopic signatures, we sampled a snapshot of 52 points evenly distributed over
206 a 200 m grid around the Vollnkirchener Bach (Fig. 1d). Soil samples were taken at four
207 consecutive rainless days (1 to 4 November 2011) at elevations of 235–294 m a.s.l.. Sampling
208 sites were selected via a stratified, GIS-based sampling plan (ArcGIS, Arc Map 10.2.1, Esri,
209 California, USA), including three classes of topographic wetness indices (TWIs: 4.4–6.5; 6.5–
210 7.7; 7.7–18.4), two different distances to stream (0–121 m, 121–250 m), and three land uses
211 (arable land, forest, and grassland), with each class containing the same number of sampling
212 points. Samples were collected at depths of 0.2 m and 0.5 m. Gravimetric water content was
213 measured according to DIN-ISO 11465 by drying soils for 24 h at 110 °C. Soil pH was analysed
214 following DIN-ISO 10390 on 1:1 soil-water-mixture with a handheld pH-meter (WTW
215 cond340i, WTW Inc., DE). Bulk density was determined according to DIN-ISO 11272, and soil
216 texture by finger testing.

217 **2.3.2 Seasonal isotope soil profiling and isotope analysis**

218 In order to trace the seasonal development of stable water isotopes from rainfall to groundwater,
219 seven soil profiles were taken in the dry summer season (28 August 2011), seven in the wet
220 winter period (28 March 2013), and two profiles in spring (24 April 2013) under different
221 vegetation cover (arable land and grassland) (Fig. 1d). Soil was sampled utilising a hand-auger
222 (Eijkelpkamp Agrisearch Equipment BV, Giesbeek, DE) from the soil surface to 2 m depth.
223 Samples were collected in greater detail near the soil surface since this area is known to have
224 the greatest isotopic variability (Barnes and Allison, 1988).

225 Soil samples were stored in amber glass tubes, sealed with Parafilm®, and kept frozen until
226 water extraction. Soil water was extracted cryogenically with 180 min extraction duration, a
227 vacuum threshold of 0.3 Pa, and an extraction temperature of 90°C following Orłowski et al.
228 (2013). Isotopic signatures of $\delta^{18}\text{O}$ and $\delta^2\text{H}$ were analysed via off-axis integrated cavity output
229 spectroscopy (OA-ICOS) (DLT-100, Los Gatos Research Inc., Mountain View, USA). Within

230 each isotope analysis three calibrated stable water isotope standards of different water isotope
231 ratios were included (LGR working standard number 1, 3, and 5; Los Gatos Research Inc., CA,
232 US). After every fifth sample the LGR working standards are measured. For each sample, six
233 sequential 900 μL aliquot of a water sample are injected into the analyser. Then, the first three
234 measurements are discarded. The remaining are averaged and corrected for per mil scale
235 linearity following the IAEA laser spreadsheet template (Newman et al., 2009). Following this
236 IAEA standard procedure allows for drift and memory corrections. Isotopic ratios are reported
237 in per mil (‰) relative to Vienna Standard Mean Ocean Water (VSMOW) (Craig, 1961b).
238 Accuracy of analyses was 0.6‰ for $\delta^2\text{H}$ and 0.2‰ for $\delta^{18}\text{O}$ (LGR, 2013). Leaf water extracts
239 typically contain a high fraction of organic contaminations, which might lead to spectral
240 interferences when using isotope ratio infrared absorption spectroscopy, causing erroneous
241 isotope values (Schultz et al., 2011). However, for soil water extracts there exists no need to
242 check or correct such data (Schultz et al., 2011; Zhao et al., 2011).

243 **2.4 Mean transit time estimation**

244 To understand the connection between the different water cycle components in the
245 Schwingbach catchment, mean transit times (MTT) for both streams as well as from
246 precipitation to groundwater were calculated using FlowPC (Maloszewski and Zuber, 2002).
247 See Appendix I for details about the applied method.

248 **2.5 Model-based groundwater age dynamics**

249 To estimate the age dynamics of the groundwater body in the Vollnkirchener Bach
250 subcatchment, a hydrological model was established on the basis of the conceptual model
251 presented by Orłowski et al. (2014) and the isotopic measurements presented here. Appendix
252 II outlines the modelling concept, model set up, and its parameterization.

253 **2.6 Statistical analyses**

254 For statistical analyses, we used IBM SPSS Statistics (Version 22, SPSS Inc., Chicago, IL, US)
255 and R (version Rx64 3.2.2). The R package igraph was utilized for plotting (Csardi and Nepusz,
256 2006). Studying temporal and spatial variations in meteoric and groundwater, isotope data were
257 tested for normal distribution. Subsequently, t-tests or Multivariate Analyses of Variances
258 (MANOVAs) were applied and Tukey-HSD tests were run to determine which groups were

259 significantly different ($p \leq 0.05$). Event mean values of isotopes in precipitation, stream, and
260 groundwater were calculated when no spatial variation was observed. Regression analyses were
261 run to determine the effect of small-scale characteristics such as distance to stream, TWI, and
262 land use on soil isotopic signatures.

263 We used a topology inference network map (Kolaczyk, 2014) in combination with a principal
264 component analysis to show $\delta^{18}\text{O}$ isotope relationships between surface and groundwater
265 sampling points. To explore the sensitivity of missing data, we used both the complete isotope
266 time series and randomly selected 80% of the whole data sets. Overall, the cluster relationships
267 of the surface and groundwater sampling points are largely similar for both whole and subsets
268 of isotope data sets, despite some differences of the exact cluster centroid locations. We
269 therefore decided to use randomly selected 80% of the isotope time series to illustrate our
270 results. In the network map, each node of the network represents an isotope sampling point.
271 The locations of the nodes are based on the first two components (PC1 and PC2). The
272 correlations between isotope time series are represented by the edges connecting nodes. The
273 thickness of edges characterizes the strength of the correlations. The p-values of correlations
274 are approximated by using the F-distributions and mid-ranks are used for the ties (Hollander et
275 al., 2013). Only statistically significant connections ($p < 0.05$) are shown.

276 To compare different water sources on the catchment-scale, a local meteoric water (LMWL)
277 line was developed and evaporation water lines (EWLs) were used. They represent the linear
278 relationship between $\delta^2\text{H}$ and $\delta^{18}\text{O}$ of meteoric waters (Cooper, 1998) in contrast to the global
279 meteoric water line (GMWL), which describes the world-wide average stable isotopic
280 composition in precipitation (Craig, 1961a). Identifying the origin of water vapour sources and
281 moisture recycling (Gat et al., 2001; Lai and Ehleringer, 2011), the deuterium-excess (d-
282 excess), defined by Dansgaard (1964) as $d = \delta^2\text{H} - 8 \times \delta^{18}\text{O}$ was used.

283 For comparisons, precipitation isotope data from the closest GNIP (Global Network of Isotopes
284 in Precipitation) station Koblenz (DE; 74 km SW of the study area, 97 m a.s.l.) was used (IAEA,
285 2014; Stumpp et al., 2014). For monthly comparisons with Schwingbach d-excess values, we
286 used a data set from the GNIP station Koblenz that includes 24 values starting from July 2011
287 to July 2013.

289 **3.1 Variations of precipitation isotopes and d-excess**

290 The $\delta^2\text{H}$ values of all precipitation isotope samples ranged from -167.6 to -8.3‰ (Table 1). To
291 examine the spatial isotopic variations, rainfall was collected at 15 open field site locations
292 throughout the Schwingbach main catchment (Fig. 1b–c) for a 7-month period, but no spatial
293 variation could be observed. Thus, rainfall was collected at the catchment outlet (site 13) from
294 23 October 2014 onward. We could neither identify an amount effect nor an altitude effect in
295 our precipitation isotope data. The greatest altitudinal difference between sampling points was
296 also only 101 m. Nevertheless, a slight temperature effect ($R^2=0.5$ for $\delta^2\text{H}$ and $R^2=0.6$ for $\delta^{18}\text{O}$,
297 respectively) was observed showing enriched isotopic signatures at higher temperatures.

298 [Table 1 near here]

299 Strong temporal variations in precipitation isotopic signatures, as well as pronounced seasonal
300 isotopic effects were measured with greatest isotopic differences occurring between summer
301 and winter. Samples taken in the fall and spring were isotopically similar, however, differed
302 from winter isotopic signature, which were somewhat lighter (Fig. 2). Furthermore, in the
303 winter of 2012–13 snow was sampled, which decreased the mean winter isotopic values for this
304 period in comparison to the previous winter period (2011–12) where no snow sampling could
305 be conducted. The mean $\delta^2\text{H}$ isotope values of snow samples were approximately 84‰ lighter
306 than mean precipitation isotopic signatures (Fig. 3). Furthermore, no statistically significant
307 ($p>0.05$) inter-annual variation was detected between the summer periods of 2011 and 2012
308 (Fig. 2).

309 [Figure 2 near here]

310 Examining the influence of moisture recycling on the isotopic compositions of precipitation,
311 the d-excess was calculated for each individual rain event at the Schwingbach catchment. D-
312 excess values ranged from -7.8‰ to $+19.4\text{‰}$ and averaged $+7.1\text{‰}$ (Fig. 2). In general, 37% of
313 all events were sampled in summer periods (21 June to 21/22 September). These summer events
314 showed lower d-excess values in comparison to the 19% winter precipitation events (21/22
315 December to 19/20 March) (Fig. 2). D-excess greater than $+10\text{‰}$ was determined for 22% of
316 all events. Lowest values corresponded to summer precipitation events where evaporation of
317 the raindrops below the cloud base may occur. Most of the higher values ($>+10\text{‰}$) appeared in

318 cold seasons (fall/winter) and winter snow samples of the Schwingbach catchment with much
319 depleted δ -values showed highest d-excess (Fig. 2).

320 In comparison with the GNIP station Koblenz (2011–2013), the mean annual d-excess at the
321 Schwingbach catchment was on average 3.9‰ higher, showing a greater impact of oceanic
322 moisture sources than the further south-west located station Koblenz. The long-term mean d-
323 excess was 4.4‰ for the Koblenz station (1978–2009) (Stumpp et al., 2014). Highest d-
324 excesses at the GNIP station matched highest values in the Schwingbach catchment, both
325 occurring in the cold seasons (October to December 2011 and November to December 2012).

326 The linear relationship of $\delta^2\text{H}$ and $\delta^{18}\text{O}$ content in local precipitation, results in a local meteoric
327 water line (LMWL) (Fig. 3). The slope of the Schwingbach LMWL is well in agreement with
328 the one from the GNIP station Koblenz ($\delta^2\text{H}=7.66\times\delta^{18}\text{O}+2.0\text{‰}$; $R^2=0.97$; 1978–2009 (Stumpp
329 et al., 2014)), but is slightly lower in comparison to the GMWL, showing stronger local
330 evaporation conditions. Since evaporation causes a differential increase in $\delta^2\text{H}$ and $\delta^{18}\text{O}$ values
331 of the remaining water, the slope for the linear relationship between $\delta^2\text{H}$ and $\delta^{18}\text{O}$ is lower in
332 comparison to the GMWL (Rozanski et al., 2001; Wu et al., 2012).

333 [Figure 3 near here]

334 **3.2 Isotopes of soil water**

335 **3.2.1 Spatial variability**

336 Determining the impact of landscape characteristics on soil water isotopic signatures, we found
337 no statistically significant connection between the parameters distance to stream, TWI, soil
338 water content, soil texture, pH, and bulk density with the soil isotopic signatures in both soil
339 depths, except for land use.

340 [Table 2 near here]

341 The mean δ -values in the top 0.2 m of the soil profile are higher than in the subsoil, reflecting
342 a stronger impact of precipitation in the topsoil (Table 2, Fig. 4). While the δ -values for subsoil
343 and precipitation differed significantly ($p\leq 0.05$), they did not for topsoil (Fig. 4). Subsoil
344 isotopic values were statistically equal to stream water and groundwater (Fig. 4).

345 [Figure 4 near here]

346 Generally, all soil water isotopic values fell on the LMWL, indicating no evaporative
347 enrichment (Fig. 5). Comparing soil isotopic signatures between different land covers showed
348 generally higher and statistically significantly different δ -values ($p \leq 0.05$) at 0.2 m soil depth
349 under arable land as compared to forests and grasslands. For the lower 0.5 m of the soil column,
350 isotopic signatures under all land uses showed statistically similar values. Comparing soil water
351 $\delta^2\text{H}$ values between top and subsoil under different land use units showed significant
352 differences ($p \leq 0.05$) under arable and grassland but not under forested sites (Fig. 5).

353 [Figure 5 near here]

354 **3.2.2 Seasonal isotope soil profiling**

355 Isotope compositions of soil water varied seasonally: More depleted soil water was found in
356 the winter and spring (Fig. 6); contrary, soil water was enriched in summer due to evaporation
357 during warmer and drier periods (Darling, 2004). For summer soil profiles in the Vollnkirchener
358 subcatchment, no evidence for evaporation was obvious below 0.4 m soil depth. However,
359 snowmelt isotopic signatures could be traced down to a soil depth of 0.9 m during spring rather
360 than winter, pointing to a depth-translocation of meltwater in the soil, more remarkable for the
361 deeper profile under arable land (Fig. 6, upper left panel). Furthermore, shallow soil water (<0.4
362 m) showed larger standard deviations with values closer to mean seasonal precipitation inputs
363 (Fig. 6, upper panels). Winter profiles exhibited somewhat greater standard deviations in
364 comparison to summer isotopic soil profiles. The observed seasonal amplitude became less
365 pronounced with depth as soil water isotope signals approached groundwater average in >0.9 m
366 depth. Generally, deeper soil water isotope values were relatively constant through time and
367 space.

368 [Figure 6 near here]

369 **3.3 Isotopes of stream water**

370 No statistically significant differences were found between the Schwingbach and
371 Vollnkirchener Bach stream water (Fig. 7). All stream water isotope samples fell on the LMWL
372 except for few evaporatively enriched samples (Fig. 3). $\delta^{18}\text{O}$ values varied for the
373 Vollnkirchener Bach by $-8.4 \pm 0.4\text{‰}$ and for the Schwingbach by $-8.4 \pm 0.6\text{‰}$ (Table 1). Stream
374 water isotopic signatures were by approximately -15‰ in $\delta^2\text{H}$ more depleted than precipitation
375 signatures and similar to groundwater (Table 1).

377 A damped seasonality of the isotope concentration in stream water versus precipitation was
378 occurring between summer and winter (Fig. 7). Most outlying depleted stream water isotopic
379 signatures (e.g. in March 2012 and 2013) can be explained by snowmelt (Fig. 7). However, the
380 outlier at the Schwingbach stream water sampling site 64 (-66.7‰ for $\delta^2\text{H}$) is by 8.5‰ more
381 depleted than the two-year average of Schwingbach stream water (Table 1). Rainfall falling on
382 24 September 2012 was -31.9‰ for $\delta^2\text{H}$. This period in September was generally characterized
383 by low flow and little rainfall. Thus, little contribution of new water was observed and stream
384 water isotopic signatures were groundwater-dominated. For site 13, the outlier in May 2012
385 (-44.2‰ for $\delta^2\text{H}$) was by 13.8‰ more enriched than the average stream water isotopic
386 composition of the Vollnkirchener Bach over the two-year observation period (Table 1). A
387 runoff peak at site 13 of 0.15 mm d^{-1} and a 2.9 mm rainfall event were recorded on 23 May
388 2012. Thus, this outlier could be explained by precipitation contributing to stream flow causing
389 more enriched isotopic values in stream water, which approached average precipitation δ -values
390 (-43.9 ± 23.4).

391 MTT calculations for the Schwingbach and the Vollnkirchener Bach did not provide a good fit
392 in terms of the quality criteria sigma and model efficiency (Timbe et al., 2014) ($\text{ME}_{\text{Schwingbach}}$
393 -0.1 – 0.0 , $\text{ME}_{\text{Vollnkirchener Bach}}$ 0.0 – 0.4 ; sigma for all sampling points 0.1). Bias correction of the
394 input data did not improve the model outputs (sigma= 0.1).

395 **3.4 Isotopes of groundwater**

396 For the piezometers under meadow, almost constant isotopic values (Fig. 8, Table 1) were
397 observed ($\delta^2\text{H}$: $-57.6 \pm 1.6\text{‰}$). Most depleted groundwater isotopic values ($< -80\text{‰}$ for $\delta^2\text{H}$)
398 were measured for piezometer 32 during snowmelt events in March and April 2013 as well as
399 for piezometer 27 from December 2012 to February 2013. Piezometer 32 is highly responsive
400 to rainfall-runoff events and groundwater head elevations showed significant correlations with
401 mean daily discharge at this site (Orlowski et al., 2014).

402 Groundwater under meadow differed from mean precipitation values by about -14‰ for $\delta^2\text{H}$
403 showing no evidence of a rapid transfer of rainfall isotopic signatures to the groundwater (Fig.
404 8). For the MTT estimations of the thirteen piezometers, the calculated output data did not fit
405 the observed values showing very low MEs (ME: -0.62 – -0.09 for $\delta^{18}\text{O}$ and -0.49 – 0.16 for
406 $\delta^2\text{H}$; sigma: 0.08 – 0.15 for $\delta^{18}\text{O}$ and 0.62 – 1.11 for $\delta^2\text{H}$).

407

[Figure 8 near here]

408 Due to different water flow paths of groundwater along the studied stream, we expected to find
409 distinguished groundwater isotopic signatures. In fact, we could identify spatial statistical
410 differences between grassland and arable land groundwater isotopic signatures (Fig. 9).
411 Groundwater isotopic signatures under arable land (sites: 25–29, Fig. 1b) showed more
412 enriched values (Fig. 8) and showed significant correlations ($p < 0.05$) among each other (Fig.
413 9). Arable land groundwater plotted furthest away from surface water sampling points in our
414 network map showing no significant correlations to either the Schwingbach or the
415 Vollnkirchener Bach. $\delta^{18}\text{O}$ time series of piezometers along the stream and under the meadow
416 showed closest relations to surface water sampling points (Fig. 9). We further found high
417 correlations ($R^2 > 0.6$) of $\delta^{18}\text{O}$ time series of piezometers located under the meadow among each
418 other. Additionally, $\delta^{18}\text{O}$ values of piezometer 3 correlated significantly ($p < 0.05$) with surface
419 water sampling points 18 and 94 ($R^2 = 0.6$ and 0.8 , respectively) and piezometer 32 with
420 sampling points 13 and 64 ($R^2 = 0.8$ and 0.6 , respectively).

421

[Figure 9 near here]

422 We further observed close relations ($p < 0.05$) among $\delta^{18}\text{O}$ values of Vollnkirchener Bach
423 sampling sites 13, 18, and 94 as well as of Schwingbach sites 11, 19, and 64 along with
424 significant correlations between each other.

425 **3.5 Groundwater age dynamics**

426 Since MTT calculations did not provide a good fit between the observed and calculated output
427 data, we modelled the groundwater age in the Vollnkirchener Bach subcatchment using CMF
428 (Appendix II), applying observed hydrometric as well as stable water isotope data (Fig. 10).

429

[Figure 10 near here]

430 The maximum age of water is highly variable throughout the subcatchment, which results in a
431 heterogeneous spatial age distribution. The groundwater in most of the outer cells is young (0–
432 10 years), whereas the inner cells, which incorporate the Vollnkirchener Bach, contain older
433 water (> 30 years). The oldest water (≥ 55 years) can be found in the Northern part of the
434 catchment (Fig. 10, detail view), where the Vollnkirchener Bach drains into the Schwingbach.
435 The main outlets of the subcatchment (dark red coloured cell and green cell) even reach an age
436 of 100 and 55 years, respectively. This can be explained by the fact that it is the lowest cell

437 within the subcatchment and that water accumulates here. The overall flow path to this cell is
438 the longest and as a consequence the groundwater age in this cell is the highest.

439 In general, 2% of cells contain groundwater that is older than 50 years, <1% reveal ages >70
440 years, 13% contain water with an age of less than one year, and 52% with an age <15 years.
441 Thus, most of the cells contain young to moderately old water (<15 years), while few cells
442 comprise old water (>50 years). The average groundwater age in the Vollnkirchener Bach
443 subcatchment is 16 years. Correlating the groundwater age against the distance to the stream,
444 we found a linear correlation ($R^2=0.3$) with a distinct trend. The water tends to be younger with
445 greater distance to the stream.

446 The amount of flowing water depicted by the length of the arrows is generally higher near the
447 stream, whereas in most of the outer cells the amount is very low (Fig. 10). The modelled main
448 flow direction is towards the Vollnkirchener Bach but many arrows show flow direction across
449 the stream indicating bidirectional water exchange between the stream and the groundwater
450 body.

451 **4 Discussion**

452 **4.1 Variations of precipitation isotopes and d-excess**

453 We found no spatial variation in precipitation isotopes throughout the Schwingbach catchment.
454 Mook et al. (1974) also observed for north-western Europe that precipitation collected over
455 periods of 8 and 24 h from three different locations within 6 km² at the same elevation were
456 consistent within 0.3‰ for $\delta^{18}\text{O}$. Further, we detected no amount or altitude effect on isotopes
457 in precipitation. Amount effects generally occur most likely in the tropics or for intense
458 convective rain events and are not a key factor for explaining isotope distributions in German
459 precipitation (Stumpp et al., 2014).

460 The observed linear relationship ($\delta^{18}\text{O}=0.44T-12.05\text{‰}$) between air temperature and
461 precipitation $\delta^{18}\text{O}$ values compares reasonably well with a correlation reported by Yurtsever
462 (1975) based on north Atlantic and European stations from the GNIP network
463 $\delta^{18}\text{O}=(0.521\pm 0.014)T-(14.96\pm 0.21)\text{‰}$. The same is true for a correlation found by Rozanski et
464 al. (1982) for the GNIP station Stuttgart, 196 km South of the Schwingbach. Stumpp et al.
465 (2014) analysed long-term precipitation data from meteorological stations across Germany and
466 found that 23 out of 24 tested stations showed a positive long-term temperature trend over time.
467 The observed correspondence between the degree of isotope depletion and the temperature

468 reflects the influence of the temperature effect in the Schwingbach catchment, which mainly
469 appears in continental, middle–high latitudes (Jouzel et al., 1997). Furthermore, the correlation
470 between $\delta^2\text{H}$ in monthly precipitations and local surface air temperature becomes increasingly
471 stronger towards the centre of the continent (Rozanski et al., 1982). Thus, the observed seasonal
472 differences in precipitation δ -values in the Schwingbach catchment could mainly be attributed
473 to seasonal differences in air temperature and the presence of snow in the winter of 2012–13
474 (Fig. 2).

475 Precipitation events originating from oceanic moisture show d-excess values close to +10‰
476 (Craig, 1961a; Dansgaard, 1964; Wu et al., 2012) and one of the main sources for precipitation
477 in Germany is moisture from the Atlantic Ocean (Stumpp et al., 2014). Lowest values
478 corresponded to summer precipitation events where evaporation of the falling raindrops below
479 the cloud base occurs. Same observations were made by Rozanski et al. (1982) for European
480 GNIP stations. Winter snow samples of the Schwingbach catchment with very depleted δ -
481 values showed highest d-excess values ($>+10\%$), well in agreement with results of Rozanski et
482 al. (1982) for European GNIP stations. The observed differences in d-excess values between
483 the Schwingbach catchment and the GNIP station Koblenz can be attributed to differences in
484 elevation range and the different regional climatic settings at both sites (Koblenz is located in
485 the relatively warmer Rhine river valley).

486 **4.2 Isotopes of soil water**

487 **4.2.1 Spatial variability**

488 We found no statistically significant connection between the parameters distance to stream,
489 TWI, soil water content, soil texture, pH, and bulk density with the soil isotopic signatures in
490 both soil depths. This was potentially attributed to the small variation in soil textures (mainly
491 clayey silts and loamy sandy silts), bulk densities, and pH values for both soil depths (Table 2).
492 Garvelmann et al. (2012) obtained high resolution $\delta^2\text{H}$ vertical depth profiles of pore water at
493 various points along two fall lines of a pasture hillslope in the Black Forest (Germany) by
494 applying the $\text{H}_2\text{O}(\text{liquid})\text{--}\text{H}_2\text{O}(\text{vapor})$ equilibration laser spectroscopy method. The authors
495 showed that groundwater was flowing through the soil in the riparian zone (downslope profiles)
496 and dominated streamflow during baseflow conditions. Their comparison indicated that the
497 percentage of pore water soil samples with a very similar stream water $\delta^2\text{H}$ signature is
498 increasing towards the stream channel (Garvelmann et al., 2012). In contrast, we found no such

499 relationship between the distance to stream or TWI and soil isotopic values in the
500 Vollnkirchener Bach subcatchment over various elevations (235–294 m a.s.l.) and locations.
501 We attributed this to the gentle hillslopes and the low subsurface flow contribution in large
502 parts of the catchment.

503 In our study, the δ -values of top soil and precipitation did not differ statistically (Fig. 4), but for
504 precipitation and subsoil they did. The latter indicates either the influence of evaporation in the
505 topsoil or the mixing with groundwater in the subsoil. However, a mixing and homogenization
506 of new and old soil water with depth could not clearly be seen in 0.5 m soil depth, which would
507 have resulted in a lower standard deviation (Song et al., 2011), but standard deviations of
508 isotopic signatures in top and subsoil were similar (Table 2). Subsoil isotopic values were
509 statistically equal to stream water and groundwater (Fig. 4) implying that capillary rise of
510 groundwater occurred. Overall, the rainfall isotopic signal was not directly transferred through
511 the soil to the groundwater; even so groundwater head level rose promptly after rainfall events.
512 This behaviour reflects the differences of celerity and velocity in the catchment's rainfall-runoff
513 response (McDonnell and Beven, 2014).

514 Soil water $\delta^2\text{H}$ between top and subsoil showed significant differences ($p \leq 0.05$) under arable
515 and grassland but not under forested sites (Fig. 5). This could be explained through the
516 occurrence of vertical preferential flow paths and interconnected macropore flow (Buttle and
517 McDonald, 2002) characteristic for forested soils. Alaoui et al. (2011) showed that macropore
518 flow with high interaction with the surrounding soil matrix occurred in forest soils, while
519 macropore flow with low to mixed interaction with the surrounding soil matrix dominates in
520 grassland soils. Seasonal tilling prevents the establishment of preferential flow paths under
521 agricultural sites and is regularly done in the Schwingbach catchment, whereas the structure of
522 forest soils, may remain uninterrupted throughout the entire soil profile for years (in particular
523 the macropores and biopores) (Alaoui et al., 2011). This is reflected in the bulk density of the
524 soils in the Schwingbach catchment that increases from forests (1.10 g cm^{-3}) over grassland
525 (1.25 g cm^{-3}) to arable land (1.41 g cm^{-3}) in the top soil. We infer that reduced hydrological
526 connection between top and subsoil under arable and grassland led to different isotopic
527 signatures (Fig. 5).

528 Although, vegetation cover has often shown an impact on soil water isotopes (Gat, 1996), only
529 few data are available for Central Europe (Darling, 2004). Burger and Seiler (1992) found that
530 soil water isotopic enrichment under spruce forest in Upper Bavaria was double that beneath

531 neighbouring arable land but soil isotope values were not comparable to groundwater (Burger
532 and Seiler, 1992). Gehrels et al. (1998) also detected (though only slightly) heavier isotopic
533 signatures under forested sites in the Netherlands in comparison to non-forested sites (grassland
534 and heathland). Contrasting, in southern Germany Brodersen et al. (2000) observed only a
535 negligible effect of throughfall isotopic signatures (of spruce and beech) on soil water isotopes,
536 since soil water in the upper layers followed the seasonal trend in the precipitation input and
537 had a very constant signature in greater depth. In a study by Sprenger et al. (2016b) the
538 differences between the investigated soil profiles across the Atert catchment (LU) were mostly
539 driven by soil types which was also seen in the pore water stable isotope dynamics reported for
540 soils in the Scottish Highlands (Geris et al., 2015). However, ~~F~~for the Schwingbach catchment
541 we conclude that the observed land use effect in the upper soil column is mainly attributed to
542 different preservation and transmission of the precipitation input signal. It is most likely not
543 attributable to distinguished throughfall isotopic signatures, impact of evaporation or
544 interception losses, since top soil water isotopic signals followed the precipitation input signal
545 under all land use units.

546 **4.2.2 Seasonal isotope soil profiling**

547 Soil water was enriched in summer due to evaporation during warmer and drier periods. The
548 depth to which soil water isotopes are significantly affected by evaporation is rarely more than
549 1–2 m below ground, and often less under temperate climates (Darling, 2004). In contrast,
550 winter profiles exhibited somewhat greater standard deviations in comparison to summer
551 isotopic soil profiles, indicative for wetter soils (Fig. 6, lower panels) and shorter residence
552 times (Thomas et al., 2013). Isotope profiles taken during or after snow melt in a study by
553 Sprenger et al. (2016b) did not show an isotopic depletion at a certain depth as observed for
554 example by Stumpp and Hendry (2012) and Peralta-Tapia et al. (2015). Generally, deeper soil
555 water isotope values in our study were relatively constant through time and space. Similar
556 findings were made by Foerstel et al. (1991) on a sandy soil in western Germany, McConville
557 et al. (2001) under predominately agriculturally used Ggley and till soils in Northern Ireland,
558 ~~and~~ Thomas et al. (2013) in a forested catchment in central Pennsylvania, USA, and Bertrand
559 et al. (2014) on the Pfynd alluvial forest (CH). Furthermore, Tang and Feng (2001) showed for
560 a sandy loam in New Hampshire (USA) that the influence of summer precipitation decreased
561 with increasing depth, and soils at 0.5 m only received water from large storms. Pore water $\delta^2\text{H}$
562 profiles taken at the catchment of the groundwater aquifer Freiburger Bucht (DE) in a study by

563 Sprengrer et al. (2016a) showed how the isotopic signal of rain water over time is preserved in
564 the unsaturated soil profile. However, the input signal was dampened due to mixing processes.
565 In our summer soil profiles under arable land, precipitation input signals ~~similarly~~ decreased
566 with depth (Fig. 6, upper left panel). Dampening of precipitation's isotopic fluctuations with
567 increasing soil depth was in line with other studies (e.g. Muñoz-Villers and McDonnell, 2012;
568 Timbe et al., 2014; Wang et al., 2010). Generally, the replacement of old soil water with new
569 infiltrating water is dependent on the frequency and intensity of precipitation and the soil
570 texture, structure, wetness, and water potential of the soil (Li et al., 2007; Tang and Feng, 2001).
571 As a result, the amount of percolating water decreases with depth and consequently, deeper soil
572 layers have less chance to obtain new water (Tang and Feng, 2001). In the growing season, the
573 percolation depth is additionally limited by plants' transpiration (Tang and Feng, 2001). For the
574 Schwingbach catchment we conclude that the percolation of new soil water is low as no
575 remarkable seasonality in soil isotopic signatures was obvious at >0.9 m and constant values
576 were observed through space and time. Although replications over several years are missing,
577 this result indicates a transit time through the rooting zone (1m) of approximately one year.

578 **4.3 Linkages between water cycle components**

579 Stream water isotopic time series of the Vollnkirchener Bach and Schwingbach showed little
580 deflections through time. Due to the observed isotopic similarities of stream and groundwater,
581 we conclude that groundwater predominantly feeds baseflow (discharge <10 L·s⁻¹). Even
582 during peak flow occurring in January 2012, December to April or May 2013, rainfall input did
583 not play a major role for stream water isotopic composition although fast rainfall-runoff
584 behaviours were observed by Orłowski et al. (2014). The damped groundwater isotopic
585 signatures seemed to be a mixture of former lighter precipitation events and snowmelt, since
586 meltwater is known to be depleted in stable isotopes as compared to precipitation or
587 groundwater (Rohde, 1998) (Figure 3). However, differences in the snow sampling method
588 (new snow, snow pit layers, meltwater) can affect the isotopic composition (Penna et al., 2014;
589 Taylor et al., 2001). As groundwater at the observed piezometers in the Vollnkirchener
590 subcatchment is shallow (Orłowski et al., 2014), the snowmelt signal is able to move rapidly
591 through the soil. Pulses of snowmelt water causing a depletion in spring and early summer was
592 also observed by other studies (Darling, 2004; Kortelainen and Karhu, 2004). We therefore
593 conclude that groundwater is mainly recharged throughout the winter. During spring runoff
594 when soils are saturated, temperatures are low, and vegetation is inactive, recharge rates are

595 generally highest. In contrast, recharge is very low during summer when most precipitation is
596 transpired back to the atmosphere (Clark and Fritz, 1997a). Similarly, O'Driscoll et al. (2005)
597 showed that summer precipitation does not significantly contribute to recharge in the Spring
598 Creek watershed (Pennsylvania, USA) since $\delta^{18}\text{O}$ values in summer precipitation were enriched
599 compared to mean annual groundwater composition.

600 Further, Orlowski et al. (2014) showed that influent and effluent conditions (bidirectional water
601 exchange) occurred simultaneously at different stream sections of the Vollnkirchener Bach
602 affecting stream and groundwater isotopic compositions, equally. Our network map supported
603 this assumption (Fig. 9) as surface water sampling points plotted close to groundwater sampling
604 points (especially to the sampling points under the meadow and along the stream). This was
605 also underlined by our groundwater model showing flow directions across the Vollnkirchener
606 Bach. Nevertheless, both stream and groundwater differed significantly from rainfall isotopic
607 signatures (Table 1). Thus, our catchment showed double water paradox behaviour as per
608 Kirchner (2003) with fast release of very old water but little variation in tracer concentration.

609 **4.4 Water age dynamics**

610 Our MTT calculations did not provide a good fit between the observed and calculated data. Just
611 by comparing mean precipitation, stream, and groundwater isotopic signatures (Table 1), one
612 could expect that simple mixing calculations would not work to derive MTTs, i.e. showing
613 predominant groundwater contribution. Same observations were made by Jin et al. (2010)
614 indicating good hydraulic connectivity between surface water and shallow groundwater. Just as
615 in the here presented results, Klaus et al. (2015) had difficulties to apply traditional methods of
616 isotope hydrology (MTT estimation, hydrograph separation) to their dataset due to the lack of
617 temporal isotopic variation in stream water of a forested low-mountainous catchment in South
618 Carolina (USA). Furthermore, stable water isotopes can only be utilised for estimations of
619 younger water (<5 years) (Stewart et al., 2010) as they are blind to older contributions (Duvert
620 et al., 2016). In our catchment, transit times are orders of magnitudes longer than the timescale
621 of hydrologic response (prompt discharge of old water) (McDonnell et al., 2010) and the range
622 used for stable water isotopes.

623 Accurately capturing the transit time of the old water fraction is essential (Duvert et al., 2016)
624 and could previously only be determined via other tracers such as tritium (e.g. Michel (1992)).
625 Current studies on mixing assumptions either consider spatial or time-varying MTTs.

626 Heidbüchel et al. (2012) proposed the concept of the master transit time distribution that
627 accounts for the temporal variability of MTT. The time-varying transit time concept of Botter
628 et al. (2011) and van der Velde et al. (2012), was recently reformulated by Harman (2015) so
629 that the storage selection function became a function of the watershed storage and actual time.
630 Instead of quantifying time-variant travel times, our model facilitates the estimation of spatially
631 distributed groundwater ages, which opens up new opportunities to compare groundwater ages
632 from over a range of scales within catchments. It further gives a deeper understanding of the
633 groundwater-surface water connection across the landscape than a classical MTT calculation
634 could provide. Our work complements recent advances in spatially distributed modelling of age
635 distributions through transient groundwater flows (e.g. Gomez and Wilson, 2013; Woolfenden
636 and Ginn, 2009). The results of our model reveal a spatially highly heterogeneous age
637 distribution of groundwater throughout the Vollnkirchener Bach subcatchment (ages of 2 days–
638 100 years) with oldest water near the stream. Thus, our model provides the opportunity to make
639 use of stable water isotope information along with climate, land use, and soil type data, in
640 combination with a digital elevation map to estimate residence times >5 years. If stable water
641 isotope information is used alone, it is known to cause a truncation of stream residence time
642 distributions (Stewart et al., 2010). Further, our groundwater model suggests that the main
643 groundwater flow direction is towards and across the stream and the quantity of flowing water
644 is highest near the stream (Fig. 10). This further supports the assumption that stream water is
645 mainly fed by older groundwater. Moreover, the simulation underlines the conclusion that the
646 groundwater body and stream water are isotopically disconnected from the precipitation cycle,
647 since only 13% of cells contained water with and age <1 year.

648 However, our semi-conceptual model approach has also some limitations. During model setup
649 a series of assumptions and simplifications were made to develop a realistic hydrologic model
650 without a severe loss in performance. Due to the assumption of a constant groundwater recharge
651 over the course of a year, no seasonality was simulated. Moreover, no spatial differences in soil
652 properties of the groundwater layer were considered. Further, several parameters such as the
653 depth of the groundwater body are only rough estimations, while others like evapotranspiration
654 are based on simulations. Moreover, the groundwater body is highly simplified since e.g.
655 properties of the simulated aquifer are assumed to be constant over the subcatchment.
656 Nevertheless, as shown by the diverse ages of water in the stream cells and the assumption of
657 spatially gaining conditions, the model confirms that the stream contains water with different
658 transit times and supports the assumption that surface and groundwater are isotopically

659 disconnected from precipitation. Therefore, the stream water does not have a discrete age, but
660 a distribution of ages due to variable flow paths (Stewart et al., 2010). In future models a more
661 diverse groundwater body based on small-scale measurements of aquifer parameters should be
662 implemented. Especially data of saturated hydraulic conductivity with high spatial resolution,
663 as well as the implementation of a temporal dynamic groundwater recharge could lead to an
664 enhanced model performance.

665 **5 Conclusions**

666 Conducting a stable water isotope study in the Schwingbach catchment helped to identify
667 relationships between precipitation, stream, soil, and groundwater in a developed (managed)
668 catchment. The close isotopic link between groundwater and the streams revealed that
669 groundwater controls streamflow. Moreover, it could be shown that groundwater was
670 predominately recharged during winter but was decoupled from the annual precipitation cycle.
671 Even so streamflow and groundwater head levels promptly responded to precipitation inputs,
672 there was no obvious change in their isotopic composition due to rain events.

673 Nevertheless, the lack of temporal variation in stable isotope time series of stream and
674 groundwater limited the application of classical methods of isotope hydrology, i.e. transfer
675 function based MTT estimations. By splitting the flow path into different compartments (upper
676 and lower vadose zone, groundwater, stream), we were able to determine, where the water age
677 passes the limit of using stable isotopes for age calculations. This limit is in the lower vadose
678 zone approximately 1–2 m below ground. To estimate the total transit time to the stream, we
679 set up a hydrological model calculating spatially distributed groundwater ages and flow
680 directions in the Vollnkirchener Bach subcatchment. Our model results supported the finding
681 that the water in the catchment is >5 years (on average 16 years) and that stream water is mainly
682 fed by groundwater. Our modelling approach was valuable to overcome the limitations of MTT
683 calculations with traditional methods and/or models. Further, our dual isotope study in
684 combination with the hydrological model approach enabled the determination of connection
685 and disconnection between different water cycle components.

686 **Acknowledgements**

687 The first author acknowledges financial support by the Friedrich-Ebert-Stiftung (Bonn, DE).
688 Furthermore, this work was supported by the Deutsche Forschungsgemeinschaft under Grant
689 BR2238/10-1. Thanks also to the student assistants, BSc. and MSc. students for their help
690 during field sampling campaigns and hydrological modelling. In this regard we like to

691 acknowledge especially Julia Mechsner, Julia Klöver, and Judith Henkel. We thank Dr.
692 Christine Stumpp from the Helmholtz Zentrum München for providing us the isotope data from
693 GNIP station Koblenz.
694

695 **References**

- 696 [Alaoui, A., Caduff, U., Gerke, H. H. and Weingartner, R.: Preferential Flow Effects on](#)
697 [Infiltration and Runoff in Grassland and Forest Soils, *Vadose Zone J.*, 10\(1\), 367,](#)
698 [doi:10.2136/vzj2010.0076, 2011.](#)
- 699 [Allan, J. D.: Landscapes and Riverscapes: The Influence of Land Use on Stream Ecosystems,](#)
700 [*Annu. Rev. Ecol. Evol. Syst.*, 35, 257–284, doi:10.1146/annurev.ecolsys.35.120202.110122,](#)
701 [2004.](#)
- 702 [Barnes, C. J. and Allison, G. B.: Tracing of water movement in the unsaturated zone using](#)
703 [stable isotopes of hydrogen and oxygen, *J. Hydrol.*, 100\(1–3\), 143–176, doi:10.1016/0022-](#)
704 [1694\(88\)90184-9, 1988.](#)
- 705 [Barthold, F. K., Tyralla, C., Schneider, K., Vaché, K. B., Frede, H.-G. and Breuer, L.: How](#)
706 [many tracers do we need for end member mixing analysis \(EMMA\)? A sensitivity analysis,](#)
707 [*Water Resour. Res.*, 47\(8\), doi:10.1029/2011WR010604, 2011.](#)
- 708 [Bertrand, G., Masini, J., Goldscheider, N., Meeks, J., Lavastre, V., Celle-Jeanton, H., Gobat,](#)
709 [J.-M. and Hunkeler, D.: Determination of spatiotemporal variability of tree water uptake using](#)
710 [stable isotopes \(\$\delta^{18}\text{O}\$, \$\delta^2\text{H}\$ \) in an alluvial system supplied by a high-altitude watershed, *Pfyn*
711 \[forest, Switzerland, *Ecohydrol.*, 7\\(2\\), 319–333, doi:10.1002/eco.1347, 2014.\]\(#\)](#)
- 712 [Blasch, K. W. and Bryson, J. R.: Distinguishing Sources of Ground Water Recharge by Using](#)
713 [\$\delta^2\text{H}\$ and \$\delta^{18}\text{O}\$, *Ground Water*, 45\(3\), 294–308, doi:10.1111/j.1745-6584.2006.00289.x, 2007.](#)
- 714 [Botter, G., Bertuzzo, E. and Rinaldo, A.: Transport in the hydrologic response: Travel time](#)
715 [distributions, soil moisture dynamics, and the old water paradox, *Water Resour. Res.*, 46\(3\),](#)
716 [W03514, doi:10.1029/2009WR008371, 2010.](#)
- 717 [Botter, G., Bertuzzo, E. and Rinaldo, A.: Catchment residence and travel time distributions:](#)
718 [The master equation, *Geophys. Res. Lett.*, 38\(11\), L11403, doi:10.1029/2011GL047666, 2011.](#)
- 719 [Brodersen, C., Pohl, S., Lindenlaub, M., Leibundgut, C. and Wilpert, K. v: Influence of](#)
720 [vegetation structure on isotope content of throughfall and soil water, *Hydrol. Process.*, 14\(8\),](#)
721 [1439–1448, doi:10.1002/1099-1085\(20000615\)14:8<1439::AID-HYP985>3.0.CO;2-3, 2000.](#)
- 722 [Burger, H. M. and Seiler, K. P.: Evaporation from soil water under humid climate conditions](#)
723 [and its impact on deuterium and \$^{18}\text{O}\$ concentrations in groundwater, edited by International](#)
724 [Atomic Energy Agency, International Atomic Energy Agency, Vienna, Austria., 1992.](#)
- 725 [Buttle, J. M.: Isotope hydrograph separations and rapid delivery of pre-event water from](#)
726 [drainage basins, *Prog. Phys. Geogr.*, 18\(1\), 16–41, doi:10.1177/030913339401800102, 1994.](#)
- 727 [Buttle, J. M.: Isotope Hydrograph Separation of Runoff Sources, in *Encyclopedia of*](#)
728 [*Hydrological Sciences*, edited by M. G. Anderson, p. 10:116, John Wiley & Sons, Ltd,](#)
729 [Chichester, Great Britain., 2006.](#)
- 730 [Buttle, J. M. and McDonald, D. J.: Coupled vertical and lateral preferential flow on a forested](#)
731 [slope, *Water Resour. Res.*, 38\(5\), 18–1, doi:10.1029/2001WR000773, 2002.](#)
- 732 [Clark, I. D. and Fritz, P.: Groundwater, in *Environmental Isotopes in Hydrogeology*, p. 80, CRC](#)
733 [Press, Florida, FL, USA., 1997a.](#)
- 734 [Clark, I. D. and Fritz, P.: Methods for Field Sampling, in *Environmental Isotopes in*](#)
735 [*Hydrogeology*, p. 283, CRC Press, Florida, FL, USA., 1997b.](#)

736 Clark, I. D. and Fritz, P.: The Environmental Isotopes, in Environmental Isotopes in
737 Hydrogeology, pp. 2–34, CRC Press, Florida, FL, USA., 1997c.

738 Cooper, L. W.: Isotopic Fractionation in Snow Cover, in Isotope Tracers in Catchment
739 Hydrology, edited by C. Kendall and J. J. McDonnell, pp. 119–136, Elsevier, Amsterdam,
740 Netherlands., 1998.

741 Craig, H.: Isotopic Variations in Meteoric Waters, Science, 133(3465), 1702–1703,
742 doi:10.1126/science.133.3465.1702, 1961a.

743 Craig, H.: Standard for reporting concentrations of deuterium and oxygen-18 in natural waters,
744 Science, 133(3467), 1833, 1961b.

745 Csardi, G. and Nepusz, T.: The igraph software package for complex network research,
746 Complex Systems 1695. [online] Available from: <http://igraph.sf.net> (Accessed 24 December
747 2015), 2006.

748 Dansgaard, W.: Stable isotopes in precipitation, Tellus, 16(4), 436–468, doi:10.1111/j.2153-
749 3490.1964.tb00181.x, 1964.

750 Darling, W. G.: Hydrological factors in the interpretation of stable isotopic proxy data present
751 and past: a European perspective, Quat. Sci. Rev., 23(7–8), 743–770,
752 doi:10.1016/j.quascirev.2003.06.016, 2004.

753 Duvert, C., Stewart, M. K., Cendón, D. I. and Raiber, M.: Time series of tritium, stable isotopes
754 and chloride reveal short-term variations in groundwater contribution to a stream, Hydrol. Earth
755 Syst. Sci., 20(1), 257–277, doi:10.5194/hess-20-257-2016, 2016.

756 DWD: Deutscher Wetterdienst - Wetter und Klima, Bundesministerium für Verkehr und
757 digitale Infrastruktur, [online] Available from: <http://dwd.de/> (Accessed 17 February 2014),
758 2014.

759 Foerstel, H., Frinken, J., Huetzen, H., Lembrich, D. and Puetz, T.: Application of H₂¹⁸O as a
760 tracer of water flow in soil, International Atomic Energy Agency, Vienna, Austria., 1991.

761 Garvelmann, J., Kuells, C. and Weiler, M.: A porewater-based stable isotope approach for the
762 investigation of subsurface hydrological processes, Hydrol. Earth Syst. Sci., 16(2), 631–640,
763 doi:10.5194/hess-16-631-2012, 2012.

764 Gat, J. R.: Oxygen and Hydrogen Isotopes in the Hydrologic Cycle, Annu. Rev. Earth Planet.
765 Sci., 24(1), 225–262, doi:10.1146/annurev.earth.24.1.225, 1996.

766 Gat, J., R., Mook, W. G. and Meijer, H. A. J.: Environmental isotopes in the hydrological cycle:
767 Principles and Applications, edited by W. G. Mook, International Hydrological Programme;
768 United Nations Educational, Scientific and Cultural Organization and International Atomic
769 Energy Agency, Paris, France., 2001.

770 Gehrels, J. C., Peeters, J. E. M., de Vries, J. J. and Dekkers, M.: The mechanism of soil water
771 movement as inferred from ¹⁸O stable isotope studies, Hydrol. Sci. J., 43(4), 579–594,
772 doi:10.1080/02626669809492154, 1998.

773 Genereux, D. P. and Hooper, R. P.: Oxygen and Hydrogen Isotopes in Rainfall-Runoff Studies,
774 in Isotope Tracers in Catchment Hydrology, edited by C. Kendall and J. J. McDonnell, pp. 319–
775 346, Elsevier, Amsterdam, Netherlands., 1998.

776 Geris, J., Tetzlaff, D., McDonnell, J. and Soulsby, C.: The relative role of soil type and tree
777 cover on water storage and transmission in northern headwater catchments, Hydrol. Process.,
778 29(7), 1844–1860, doi:10.1002/hyp.10289, 2015.

779 Gomez, J. D. and Wilson, J. L.: Age distributions and dynamically changing hydrologic
780 systems: Exploring topography-driven flow, Water Resour. Res., 49(3), 1503–1522,
781 doi:10.1002/wrcr.20127, 2013.

782 Gonfiantini, R., Fröhlich, K., Araguás-Araguás, L. and Rozanski, K.: Isotopes in Groundwater
783 Hydrology, in Isotope Tracers in Catchment Hydrology, edited by C. Kendall and J. J.
784 McDonnell, pp. 203–246, Elsevier, Amsterdam, Netherlands., 1998.

785 Gordon, L. J., Finlayson, C. M. and Falkenmark, M.: Managing water in agriculture for food
786 production and other ecosystem services, Agric. Water Manag., 97(4), 512–519,
787 doi:10.1016/j.agwat.2009.03.017, 2010.

788 Harman, C. J.: Time-variable transit time distributions and transport: Theory and application to
789 storage-dependent transport of chloride in a watershed, Water Resour. Res., 51(1), 1–30,
790 doi:10.1002/2014WR015707, 2015.

791 Heidbüchel, I., Troch, P. A., Lyon, S. W. and Weiler, M.: The master transit time distribution
792 of variable flow systems, Water Resour. Res., 48(6), W06520, doi:10.1029/2011WR011293,
793 2012.

794 Hindmarsh, A. C., Brown, P. N., Grant, K. E., Lee, S. L., Serban, R., Shumaker, D. E. and
795 Woodward, C. S.: SUNDIALS: Suite of Nonlinear and Differential/Algebraic Equation
796 Solvers, ACM Trans. Math. Softw., 31(3), 363–396, doi:10.1145/1089014.1089020, 2005.

797 Hollander, M., Wolfe, D. A. and Chicken, E.: Nonparametric Statistical Methods, John Wiley
798 & Sons, New York, NY, USA., 2013.

799 Hrachowitz, M., Benettin, P., van Breukelen, B. M., Fovet, O., Howden, N. J. K., Ruiz, L., van
800 der Velde, Y. and Wade, A. J.: Transit times—the link between hydrology and water quality at
801 the catchment scale, Wiley Interdiscip. Rev. Water, doi:10.1002/wat2.1155, 2016.

802 IAEA: International Atomic Energy Agency: Water Resources Programme – Global Network
803 of Isotopes in Precipitation, [online] Available from: [http://www-](http://www-naweb.iaea.org/naweb/ih/IHS_resources_gnip.html)
804 naweb.iaea.org/naweb/ih/IHS_resources_gnip.html (Accessed 11 August 2014), 2014.

805 Jin, L., Siegel, D. I., Lautz, L. K., Mitchell, M. J., Dahms, D. E. and Mayer, B.: Calcite
806 precipitation driven by the common ion effect during groundwater–surface-water mixing: A
807 potentially common process in streams with geologic settings containing gypsum, Geol. Soc.
808 Am. Bull., 122(7/8), B30011.1, doi:10.1130/B30011.1, 2010.

809 Jin, L., Siegel, D. I., Lautz, L. K. and Lu, Z.: Identifying streamflow sources during spring
810 snowmelt using water chemistry and isotopic composition in semi-arid mountain streams, J.
811 Hydrol., 470–471, 289–301, doi:10.1016/j.jhydrol.2012.09.009, 2012.

812 Jouzel, J., Alley, R. B., Cuffey, K. M., Dansgaard, W., Grootes, P., Hoffmann, G., Johnsen, S.
813 J., Koster, R. D., Peel, D., Shuman, C. A., Stievenard, M., Stuiver, M. and White, J.: Validity
814 of the temperature reconstruction from water isotopes in ice cores, J. Geophys. Res., 102,
815 26471–26487, doi:10.1029/97JC01283, 1997.

816 Kendall, C. and Caldwell, E. A.: Fundamentals of Isotope Geochemistry, in Isotope Tracers in
817 Catchment Hydrology, edited by C. Kendall and J. J. McDonnell, pp. 51–86, Elsevier,
818 Amsterdam, Netherlands., 1998.

819 Kirchner, J. W.: A double paradox in catchment hydrology and geochemistry, Hydrol. Process.,
820 17(4), 871–874, doi:10.1002/hyp.5108, 2003.

821 Klaus, J., McDonnell, J. J., Jackson, C. R., Du, E. and Griffiths, N. A.: Where does streamwater

822 [come from in low-relief forested watersheds? A dual-isotope approach, Hydrol. Earth Syst.](#)
823 [Sci., 19\(1\), 125–135, 2015.](#)

824 [Koeniger, P., Leibundgut, C. and Stichler, W.: Spatial and temporal characterisation of stable](#)
825 [isotopes in river water as indicators of groundwater contribution and confirmation of modelling](#)
826 [results; a study of the Weser river, Germany, Isotopes Environ. Health Stud., 45\(4\), 289–302,](#)
827 [doi:10.1080/10256010903356953, 2009.](#)

828 [Kolaczyk, E. D.: Statistical Analysis of Network Data with R, Springer Science & Business](#)
829 [Media, New York, NY, USA., 2014.](#)

830 [Kortelainen, N. M. and Karhu, J. A.: Regional and seasonal trends in the oxygen and hydrogen](#)
831 [isotope ratios of Finnish groundwaters: a key for mean annual precipitation, J. Hydrol., 285\(1–](#)
832 [4\), 143–157, doi:10.1016/j.jhydrol.2003.08.014, 2004.](#)

833 [Kraft, P., Vaché, K. B., Frede, H.-G. and Breuer, L.: CMF: A Hydrological Programming](#)
834 [Language Extension For Integrated Catchment Models, Environ. Model. Softw., 26\(6\), 828–](#)
835 [830, doi:10.1016/j.envsoft.2010.12.009, 2011.](#)

836 [Lai, C.-T. and Ehleringer, J. R.: Deuterium excess reveals diurnal sources of water vapor in](#)
837 [forest air, Oecologia, 165\(1\), 213–223, doi:10.1007/s00442-010-1721-2, 2011.](#)

838 [Lauer, F., Frede, H.-G. and Breuer, L.: Uncertainty assessment of quantifying spatially](#)
839 [concentrated groundwater discharge to small streams by distributed temperature sensing, Water](#)
840 [Resour. Res., 49\(1\), 400–407, doi:10.1029/2012WR012537, 2013.](#)

841 [LGR: Los Gatos Research, Greenhouse Gas, isotope and trace gas analyzers, \[online\] Available](#)
842 [from: <http://www.lgrinc.com/> \(Accessed 5 February 2013\), 2013.](#)

843 [Li, F., Song, X., Tang, C., Liu, C., Yu, J. and Zhang, W.: Tracing infiltration and recharge using](#)
844 [stable isotope in Taihang Mt., North China, Environ. Geol., 53\(3\), 687–696,](#)
845 [doi:10.1007/s00254-007-0683-0, 2007.](#)

846 [Maloszewski, P. and Zuber, A.: Manual on lumped parameter models used for the interpretation](#)
847 [of environmental tracer data in groundwaters, in Use of isotopes for analyses of flow and](#)
848 [transport dynamics in groundwater systems, p. 50, International Atomic Energy Agency,](#)
849 [Vienna, Austria., 2002.](#)

850 [McConville, C., Kalin, R. m., Johnston, H. and McNeill, G. w.: Evaluation of Recharge in a](#)
851 [Small Temperate Catchment Using Natural and Applied \$\delta^{18}\text{O}\$ Profiles in the Unsaturated Zone,](#)
852 [Ground Water, 39\(4\), 616–623, doi:10.1111/j.1745-6584.2001.tb02349.x, 2001.](#)

853 [McDonnell, J. J. and Beven, K.: Debates—The future of hydrological sciences: A \(common\)](#)
854 [path forward? A call to action aimed at understanding velocities, celerities and residence time](#)
855 [distributions of the headwater hydrograph, Water Resour. Res., 50\(6\), 5342–5350,](#)
856 [doi:10.1002/2013WR015141, 2014.](#)

857 [McDonnell, J. J., Sivapalan, M., Vaché, K., Dunn, S., Grant, G., Haggerty, R., Hinz, C., Hooper,](#)
858 [R., Kirchner, J., Roderick, M. L. and others: Moving beyond heterogeneity and process](#)
859 [complexity: a new vision for watershed hydrology, Water Resour. Res., 43\(7\), W07301, 2007.](#)

860 [McDonnell, J. J., McGuire, K., Aggarwal, P., Beven, K. J., Biondi, D., Destouni, G., Dunn, S.,](#)
861 [James, A., Kirchner, J., Kraft, P., Lyon, S., Maloszewski, P., Newman, B., Pfister, L., Rinaldo,](#)
862 [A., Rodhe, A., Sayama, T., Seibert, J., Solomon, K., Soulsby, C., Stewart, M., Tetzlaff, D.,](#)
863 [Tobin, C., Troch, P., Weiler, M., Western, A., Worman, A. and Wrede, S.: How old is](#)
864 [streamwater? Open questions in catchment transit time conceptualization, modelling and](#)
865 [analysis, Hydrol. Process., 24\(12\), 1745–1754, 2010.](#)

866 [McGuire, K. J. and McDonnell, J. J.: A review and evaluation of catchment transit time](#)
867 [modeling, *J. Hydrol.*, 330\(3\), 543–563, 2006.](#)

868 [Michel, R. L.: Residence times in river basins as determined by analysis of long-term tritium](#)
869 [records, *J. Hydrol.*, 130\(1\), 367–378, doi:10.1016/0022-1694\(92\)90117-E, 1992.](#)

870 [Mook, W. G., Groeneveld, D. J., Brouwn, A. E. and Ganswijk, A. J. van: Analysis of a run-off](#)
871 [hydrograph by means of natural ¹⁸O, in *Isotope techniques in groundwater hydrology*, vol. 1,](#)
872 [pp. 159–169, International Atomic Energy Agency, Vienna, Austria., 1974.](#)

873 [Muñoz-Villers, L. E. and McDonnell, J. J.: Runoff generation in a steep, tropical montane cloud](#)
874 [forest catchment on permeable volcanic substrate, *Water Resour. Res.*, 48\(9\), n/a–n/a,](#)
875 [doi:10.1029/2011WR011316, 2012.](#)

876 [Neal, C. and Rosier, P. T. W.: Chemical studies of chloride and stable oxygen isotopes in two](#)
877 [conifer afforested and moorland sites in the British uplands, *J. Hydrol.*, 115\(1–4\), 269–283,](#)
878 [doi:10.1016/0022-1694\(90\)90209-G, 1990.](#)

879 [Newman, B., Tanweer, A. and Kurtas, T.: IAEA Standard Operating Procedure for the Liquid-](#)
880 [Water Stable Isotope Analyser, *Laser Proced. IAEA Water Resour. Programme*, 2009.](#)

881 [O’Driscoll, M. A., DeWalle, D. R., McGuire, K. J. and Gburek, W. J.: Seasonal ¹⁸O variations](#)
882 [and groundwater recharge for three landscape types in central Pennsylvania, USA, *J. Hydrol.*,](#)
883 [303\(1–4\), 108–124, doi:10.1016/j.jhydrol.2004.08.020, 2005.](#)

884 [Orlowski, N., Frede, H.-G., Brüggemann, N. and Breuer, L.: Validation and application of a](#)
885 [cryogenic vacuum extraction system for soil and plant water extraction for isotope analysis, *J.*](#)
886 [Sens. Sens. Syst., 2\(2\), 179–193, doi:10.5194/jsss-2-179-2013, 2013.](#)

887 [Orlowski, N., Lauer, F., Kraft, P., Frede, H.-G. and Breuer, L.: Linking Spatial Patterns of](#)
888 [Groundwater Table Dynamics and Streamflow Generation Processes in a Small Developed](#)
889 [Catchment, *Water*, 6\(10\), 3085–3117, doi:10.3390/w6103085, 2014.](#)

890 [Penna, D., Ahmad, M., Birks, S. J., Bouchaou, L., Brenčič, M., Butt, S., Holko, L., Jeelani, G.,](#)
891 [Martínez, D. E., Melikadze, G., Shanley, J. B., Sokratov, S. A., Städtnyk, T., Sugimoto, A. and](#)
892 [Vreča, P.: A new method of snowmelt sampling for water stable isotopes, *Hydrol. Process.*,](#)
893 [28\(22\), 5637–5644, doi:10.1002/hyp.10273, 2014.](#)

894 [Peralta-Tapia, A., Sponseller, R. A., Tetzlaff, D., Soulsby, C. and Laudon, H.: Connecting](#)
895 [precipitation inputs and soil flow pathways to stream water in contrasting boreal catchments,](#)
896 [Hydrol. Process., 29\(16\), 3546–3555, doi:10.1002/hyp.10300, 2015.](#)

897 [Perry, C. and Taylor, K.: *Environmental Sedimentology*, p. 36, Blackwell Publishing, Oxford,](#)
898 [OX, UK, 2009.](#)

899 [Pierce, S. C., Kröger, R. and Pezeshki, R.: Managing Artificially Drained Low-Gradient](#)
900 [Agricultural Headwaters for Enhanced Ecosystem Functions, *Biology*, 1\(3\), 794–856,](#)
901 [doi:10.3390/biology1030794, 2012.](#)

902 [Qu, Y. and Duffy, C. J.: A semidiscrete finite volume formulation for multiprocess watershed](#)
903 [simulation, *Water Resour. Res.*, 43\(8\), W08419, doi:10.1029/2006WR005752, 2007.](#)

904 [Rinaldo, A., Benettin, P., Harman, C. J., Hrachowitz, M., McGuire, K. J., van der Velde, Y.,](#)
905 [Bertuzzo, E. and Botter, G.: Storage selection functions: A coherent framework for quantifying](#)
906 [how catchments store and release water and solutes, *Water Resour. Res.*, 51\(6\), 4840–4847,](#)
907 [doi:10.1002/2015WR017273, 2015.](#)

908 [Rohde, A.: Snowmelt-Dominated Systems, in *Isotope Tracers in Catchment Hydrology*, edited](#)

909 [by C. Kendall and J. J. McDonnell, pp. 391–433, Elsevier, Amsterdam, Netherlands., 1998.](#)

910 [Rozanski, K., Sonntag, C. and Münnich, K. O.: Factors controlling stable isotope composition](#)
911 [of European precipitation, *Tellus*, 34\(2\), 142–150, doi:10.1111/j.2153-3490.1982.tb01801.x,](#)
912 [1982.](#)

913 [Rozanski, K., Froehlich, K. and Mook, W. G.: in *Environmental isotopes in the hydrological*](#)
914 [cycle: Principles and Applications, vol. 3, International Hydrological Programme; United](#)
915 [Nations Educational, Scientific and Cultural Organization and International Atomic Energy](#)
916 [Agency, Paris, Vienna., 2001.](#)

917 [Schultz, N. M., Griffis, T. J., Lee, X. and Baker, J. M.: Identification and correction of spectral](#)
918 [contamination in \$^2\text{H}/^1\text{H}\$ and \$^{18}\text{O}/^{16}\text{O}\$ measured in leaf, stem, and soil water, *Rapid Commun.*](#)
919 [Mass Spectrom., 25\(21\), 3360–3368, doi:10.1002/rcm.5236, 2011.](#)

920 [Shuttleworth, W. J. and Wallace, J. S.: Evaporation from sparse crops-an energy combination](#)
921 [theory, *Q. J. R. Meteorol. Soc.*, 111\(469\), 839–855, doi:10.1002/qj.49711146910, 1985.](#)

922 [Sklash, M. G.: Environmental isotope studies of storm and snowmelt runoff generation, in](#)
923 [Process studies in hillslope hydrology, edited by M. G. Anderson, pp. 410–435, Wiley, New](#)
924 [York, NY, USA., 1990.](#)

925 [Sklash, M. G. and Farvolden, R. N.: The Role Of Groundwater In Storm Runoff, in](#)
926 [Developments in Water Science, vol. 12, edited by W. B. and D. A. Stephenson, pp. 45–65,](#)
927 [Elsevier, Amsterdam, Netherlands., 1979.](#)

928 [Song, X., Wang, P., Yu, J., Liu, X., Liu, J. and Yuan, R.: Relationships between precipitation,](#)
929 [soil water and groundwater at Chongling catchment with the typical vegetation cover in the](#)
930 [Taihang mountainous region, China, *Environ. Earth Sci.*, 62\(4\), 787–796, doi:10.1007/s12665-](#)
931 [010-0566-7, 2011.](#)

932 [Sprenger, M., Erhardt, M., Riedel, M. and Weiler, M.: Historical tracking of nitrate in](#)
933 [contrasting vineyards using water isotopes and nitrate depth profiles, *Agric. Ecosyst. Environ.*,](#)
934 [222, 185–192, doi:10.1016/j.agee.2016.02.014, 2016a.](#)

935 [Sprenger, M., Seeger, S., Blume, T. and Weiler, M.: Travel times in the vadose zone: Variability](#)
936 [in space and time, *Water Resour. Res.*, n/a-n/a, doi:10.1002/2015WR018077, 2016b.](#)

937 [Stewart, M. K., Morgenstern, U. and McDonnell, J. J.: Truncation of stream residence time:](#)
938 [how the use of stable isotopes has skewed our concept of streamwater age and origin, *Hydrol.*](#)
939 [Process., 24\(12\), 1646–1659, doi:10.1002/hyp.7576, 2010.](#)

940 [Stumpp, C. and Hendry, M. J.: Spatial and temporal dynamics of water flow and solute transport](#)
941 [in a heterogeneous glacial till: The application of high-resolution profiles of \$\delta^{18}\text{O}\$ and \$\delta^2\text{H}\$ in](#)
942 [pore waters, *J. Hydrol.*, 438–439, 203–214, doi:10.1016/j.jhydrol.2012.03.024, 2012.](#)

943 [Stumpp, C., Klaus, J. and Stichler, W.: Analysis of long-term stable isotopic composition in](#)
944 [German precipitation, *J. Hydrol.*, 517, 351–361, doi:10.1016/j.jhydrol.2014.05.034, 2014.](#)

945 [Tang, K. and Feng, X.: The effect of soil hydrology on the oxygen and hydrogen isotopic](#)
946 [compositions of plants' source water, *Earth Planet. Sci. Lett.*, 185\(3–4\), 355–367, 2001.](#)

947 [Taylor, S., Feng, X., Kirchner, J. W., Osterhuber, R., Klaue, B. and Renshaw, C. E.: Isotopic](#)
948 [evolution of a seasonal snowpack and its melt, *Water Resour. Res.*, 37\(3\), 759–769,](#)
949 [doi:10.1029/2000WR900341, 2001.](#)

950 [Thomas, E. M., Lin, H., Duffy, C. J., Sullivan, P. L., Holmes, G. H., Brantley, S. L. and Jin, L.:](#)
951 [Spatiotemporal Patterns of Water Stable Isotope Compositions at the Shale Hills Critical Zone](#)

952 Observatory: Linkages to Subsurface Hydrologic Processes, Vadose Zone J., 12(4), 0,
953 doi:10.2136/vzj2013.01.0029, 2013.

954 Timbe, E., Windhorst, D., Crespo, P., Frede, H.-G., Feyen, J. and Breuer, L.: Understanding
955 uncertainties when inferring mean transit times of water through tracer-based lumped-parameter
956 models in Andean tropical montane cloud forest catchments, Hydrol. Earth Syst. Sci., 18(4),
957 1503–1523, doi:10.5194/hess-18-1503-2014, 2014.

958 van der Velde, Y., Torfs, P. J. J. F., van der Zee, S. E. a. T. M. and Uijlenhoet, R.: Quantifying
959 catchment-scale mixing and its effect on time-varying travel time distributions, Water Resour.
960 Res., 48(6), W06536, doi:10.1029/2011WR011310, 2012.

961 Wang, P., Song, X., Han, D., Zhang, Y. and Liu, X.: A study of root water uptake of crops
962 indicated by hydrogen and oxygen stable isotopes: A case in Shanxi Province, China, Agric.
963 Water Manag., 97(3), 475–482, 2010.

964 Wang, X. F. and Yakir, D.: Using stable isotopes of water in evapotranspiration studies, Hydrol.
965 Process., 14(8), 1407–1421, doi:10.1002/1099-1085(20000615)14:8<1407::AID-
966 HYP992>3.0.CO;2-K, 2000.

967 Windhorst, D., Waltz, T., Timbe, E., Frede, H.-G. and Breuer, L.: Impact of elevation and
968 weather patterns on the isotopic composition of precipitation in a tropical montane rainforest,
969 Hydrol. Earth Syst. Sci., 17(1), 409–419, doi:10.5194/hess-17-409-2013, 2013.

970 Windhorst, D., Kraft, P., Timbe, E., Frede, H.-G. and Breuer, L.: Stable water isotope tracing
971 through hydrological models for disentangling runoff generation processes at the hillslope
972 scale, Hydrol. Earth Syst. Sci., 18(10), 4113–4127, doi:10.5194/hess-18-4113-2014, 2014.

973 Woelfenden, L. R. and Ginn, T. R.: Modeled Ground Water Age Distributions, Ground Water,
974 47(4), 547–557, doi:10.1111/j.1745-6584.2008.00550.x, 2009.

975 Wu, J., Ding, Y., Ye, B., Yang, Q., Hou, D. and Xue, L.: Stable isotopes in precipitation in
976 Xilin River Basin, northern China and their implications, Chin. Geogr. Sci., 22(5), 531–540,
977 doi:10.1007/s11769-012-0543-z, 2012.

978 Xia, Y.: Optimization and uncertainty estimates of WMO regression models for the systematic
979 bias adjustment of NLDAS precipitation in the United States, J. Geophys. Res. Atmospheres,
980 111(D8), D08102, doi:10.1029/2005JD006188, 2006.

981 Yurtsever, Y.: Worldwide survey of stable isotopes in precipitation, International Atomic
982 Energy Agency, Vienna, Austria., 1975.

983 Zhao, L., Xiao, H., Zhou, J., Wang, L., Cheng, G., Zhou, M., Yin, L. and McCabe, M. F.:
984 Detailed assessment of isotope ratio infrared spectroscopy and isotope ratio mass spectrometry
985 for the stable isotope analysis of plant and soil waters, Rapid Commun. Mass Spectrom., 25(20),
986 3071–3082, doi:10.1002/rcm.5204, 2011.

987 Alaoui, A., Caduff, U., Gerke, H. H. and Weingartner, R.: Preferential Flow Effects on
988 Infiltration and Runoff in Grassland and Forest Soils, Vadose Zone J., 10(1), 367,
989 doi:10.2136/vzj2010.0076, 2011.

990 Allan, J. D.: Landscapes and Riverscapes: The Influence of Land Use on Stream Ecosystems,
991 Annu. Rev. Ecol. Evol. Syst., 35, 257–284, doi:10.1146/annurev.ecolsys.35.120202.110122,
992 2004.

993 Barnes, C. J. and Allison, G. B.: Tracing of water movement in the unsaturated zone using
994 stable isotopes of hydrogen and oxygen, J. Hydrol., 100(1–3), 143–176, doi:10.1016/0022-

995 1694(88)90184-9, 1988.

996 Barthold, F. K., Tyralla, C., Schneider, K., Vaché, K. B., Frede, H. G. and Breuer, L.: How
997 many tracers do we need for end member mixing analysis (EMMA)? A sensitivity analysis,
998 *Water Resour. Res.*, 47(8), doi:10.1029/2011WR010604, 2011.

999 Blasch, K. W. and Bryson, J. R.: Distinguishing Sources of Ground Water Recharge by Using
1000 $\delta^2\text{H}$ and $\delta^{18}\text{O}$, *Ground Water*, 45(3), 294–308, doi:10.1111/j.1745-6584.2006.00289.x, 2007.

1001 Botter, G., Bertuzzo, E. and Rinaldo, A.: Transport in the hydrologic response: Travel time
1002 distributions, soil moisture dynamics, and the old water paradox, *Water Resour. Res.*, 46(3),
1003 W03514, doi:10.1029/2009WR008371, 2010.

1004 Botter, G., Bertuzzo, E. and Rinaldo, A.: Catchment residence and travel time distributions:
1005 The master equation, *Geophys. Res. Lett.*, 38(11), L11403, doi:10.1029/2011GL047666, 2011.

1006 Brodersen, C., Pohl, S., Lindenlaub, M., Leibundgut, C. and Wilpert, K. v: Influence of
1007 vegetation structure on isotope content of throughfall and soil water, *Hydrol. Process.*, 14(8),
1008 1439–1448, doi:10.1002/1099-1085(20000615)14:8<1439::AID-HYP985>3.0.CO;2-3, 2000.

1009 Burger, H. M. and Seiler, K. P.: Evaporation from soil water under humid climate conditions
1010 and its impact on deuterium and ^{18}O concentrations in groundwater, edited by International
1011 Atomic Energy Agency, International Atomic Energy Agency, Vienna, Austria., 1992.

1012 Buttle, J. M.: Isotope hydrograph separations and rapid delivery of pre-event water from
1013 drainage basins, *Prog. Phys. Geogr.*, 18(1), 16–41, doi:10.1177/030913339401800102, 1994.

1014 Buttle, J. M.: Isotope Hydrograph Separation of Runoff Sources, in *Encyclopedia of*
1015 *Hydrological Sciences*, edited by M. G. Anderson, p. 10:116, John Wiley & Sons, Ltd,
1016 Chichester, Great Britain., 2006.

1017 Buttle, J. M. and McDonald, D. J.: Coupled vertical and lateral preferential flow on a forested
1018 slope, *Water Resour. Res.*, 38(5), 18–1, doi:10.1029/2001WR000773, 2002.

1019 Clark, I. D. and Fritz, P.: Groundwater, in *Environmental Isotopes in Hydrogeology*, p. 80, CRC
1020 Press, Florida, FL, USA., 1997a.

1021 Clark, I. D. and Fritz, P.: Methods for Field Sampling, in *Environmental Isotopes in*
1022 *Hydrogeology*, p. 283, CRC Press, Florida, FL, USA., 1997b.

1023 Clark, I. D. and Fritz, P.: The Environmental Isotopes, in *Environmental Isotopes in*
1024 *Hydrogeology*, pp. 2–34, CRC Press, Florida, FL, USA., 1997c.

1025 Cooper, L. W.: Isotopic Fractionation in Snow Cover, in *Isotope Tracers in Catchment*
1026 *Hydrology*, edited by C. Kendall and J. J. McDonnell, pp. 119–136, Elsevier, Amsterdam,
1027 Netherlands., 1998.

1028 Craig, H.: Isotopic Variations in Meteoric Waters, *Science*, 133(3465), 1702–1703,
1029 doi:10.1126/science.133.3465.1702, 1961a.

1030 Craig, H.: Standard for reporting concentrations of deuterium and oxygen-18 in natural waters,
1031 *Science*, 133(3467), 1833, 1961b.

1032 Csardi, G. and Nepusz, T.: The igraph software package for complex network research,
1033 *Complex Systems* 1695. [online] Available from: <http://igraph.sf.net> (Accessed 24 December
1034 2015), 2006.

1035 Dansgaard, W.: Stable isotopes in precipitation, *Tellus*, 16(4), 436–468, doi:10.1111/j.2153-
1036 3490.1964.tb00181.x, 1964.

1037 Darling, W. G.: Hydrological factors in the interpretation of stable isotopic proxy data present
1038 and past: a European perspective, *Quat. Sci. Rev.*, 23(7-8), 743-770,
1039 doi:10.1016/j.quascirev.2003.06.016, 2004.

1040 Duvert, C., Stewart, M. K., Cendón, D. I. and Raiber, M.: Time series of tritium, stable isotopes
1041 and chloride reveal short-term variations in groundwater contribution to a stream, *Hydrol. Earth
1042 Syst. Sci.*, 20(1), 257-277, doi:10.5194/hess-20-257-2016, 2016.

1043 DWD: Deutscher Wetterdienst – Wetter und Klima, Bundesministerium für Verkehr und
1044 digitale Infrastruktur, [online] Available from: <http://dwd.de/> (Accessed 17 February 2014),
1045 2014.

1046 Foerstel, H., Frinken, J., Huetzen, H., Lembrich, D. and Puetz, T.: Application of H₂¹⁸O as a
1047 tracer of water flow in soil, International Atomic Energy Agency, Vienna, Austria., 1991.

1048 Garvelmann, J., Kuells, C. and Weiler, M.: A porewater-based stable isotope approach for the
1049 investigation of subsurface hydrological processes, *Hydrol. Earth Syst. Sci.*, 16(2), 631-640,
1050 doi:10.5194/hess-16-631-2012, 2012.

1051 Gat, J. R.: Oxygen and Hydrogen Isotopes in the Hydrologic Cycle, *Annu. Rev. Earth Planet.
1052 Sci.*, 24(1), 225-262, doi:10.1146/annurev.earth.24.1.225, 1996.

1053 Gat, J., R., Mook, W. G. and Meijer, H. A. J.: Environmental isotopes in the hydrological cycle:
1054 Principles and Applications, edited by W. G. Mook, International Hydrological Programme;
1055 United Nations Educational, Scientific and Cultural Organization and International Atomic
1056 Energy Agency, Paris, France., 2001.

1057 Gehrels, J. C., Peeters, J. E. M., de Vries, J. J. and Dekkers, M.: The mechanism of soil water
1058 movement as inferred from ¹⁸O stable isotope studies, *Hydrol. Sci. J.*, 43(4), 579-594,
1059 doi:10.1080/02626669809492154, 1998.

1060 Genereux, D. P. and Hooper, R. P.: Oxygen and Hydrogen Isotopes in Rainfall-Runoff Studies,
1061 in *Isotope Tracers in Catchment Hydrology*, edited by C. Kendall and J. J. McDonnell, pp. 319-
1062 346, Elsevier, Amsterdam, Netherlands., 1998.

1063 Gomez, J. D. and Wilson, J. L.: Age distributions and dynamically changing hydrologic
1064 systems: Exploring topography-driven flow, *Water Resour. Res.*, 49(3), 1503-1522,
1065 doi:10.1002/wrer.20127, 2013.

1066 Gonfiantini, R., Fröhlich, K., Araguás-Araguás, L. and Rozanski, K.: Isotopes in Groundwater
1067 Hydrology, in *Isotope Tracers in Catchment Hydrology*, edited by C. Kendall and J. J.
1068 McDonnell, pp. 203-246, Elsevier, Amsterdam, Netherlands., 1998.

1069 Gordon, L. J., Finlayson, C. M. and Falkenmark, M.: Managing water in agriculture for food
1070 production and other ecosystem services, *Agric. Water Manag.*, 97(4), 512-519,
1071 doi:10.1016/j.agwat.2009.03.017, 2010.

1072 Harman, C. J.: Time-variable transit time distributions and transport: Theory and application to
1073 storage-dependent transport of chloride in a watershed, *Water Resour. Res.*, 51(1), 1-30,
1074 doi:10.1002/2014WR015707, 2015.

1075 Heidebüchel, I., Troch, P. A., Lyon, S. W. and Weiler, M.: The master transit time distribution
1076 of variable flow systems, *Water Resour. Res.*, 48(6), W06520, doi:10.1029/2011WR011293,
1077 2012.

1078 Hindmarsh, A. C., Brown, P. N., Grant, K. E., Lee, S. L., Serban, R., Shumaker, D. E. and
1079 Woodward, C. S.: SUNDIALS: Suite of Nonlinear and Differential/Algebraic Equation

1080 *Solvers*, *ACM Trans. Math. Softw.*, 31(3), 363–396, doi:10.1145/1089014.1089020, 2005.

1081 Hollander, M., Wolfe, D. A. and Chicken, E.: *Nonparametric Statistical Methods*, John Wiley
1082 & Sons, New York, NY, USA., 2013.

1083 Hrachowitz, M., Benettin, P., van Breukelen, B. M., Fovet, O., Howden, N. J. K., Ruiz, L., van
1084 der Velde, Y. and Wade, A. J.: Transit times—the link between hydrology and water quality at
1085 the catchment scale, *Wiley Interdiscip. Rev. Water*, doi:10.1002/wat2.1155, 2016.

1086 IAEA: International Atomic Energy Agency: Water Resources Programme—Global Network
1087 of—Isotopes—in—Precipitation,—[online]—Available—from:—[http://www-](http://www-naweb.iaea.org/nape/ih/IHS_resources_gnip.html)
1088 [naweb.iaea.org/nape/ih/IHS_resources_gnip.html](http://www-naweb.iaea.org/nape/ih/IHS_resources_gnip.html) (Accessed 11 August 2014), 2014.

1089 Jin, L., Siegel, D. I., Lautz, L. K., Mitchell, M. J., Dahms, D. E. and Mayer, B.: Calcite
1090 precipitation driven by the common ion effect during groundwater surface water mixing: A
1091 potentially common process in streams with geologic settings containing gypsum, *Geol. Soc.
1092 Am. Bull.*, 122(7/8), B30011.1, doi:10.1130/B30011.1, 2010.

1093 Jin, L., Siegel, D. I., Lautz, L. K. and Lu, Z.: Identifying streamflow sources during spring
1094 snowmelt using water chemistry and isotopic composition in semi arid mountain streams, *J.
1095 Hydrol.*, 470–471, 289–301, doi:10.1016/j.jhydrol.2012.09.009, 2012.

1096 Jouzel, J., Alley, R. B., Cuffey, K. M., Dansgaard, W., Grootes, P., Hoffmann, G., Johnsen, S.
1097 J., Koster, R. D., Peel, D., Shuman, C. A., Stievenard, M., Stuiver, M. and White, J.: Validity
1098 of the temperature reconstruction from water isotopes in ice cores, *J. Geophys. Res.*, 102,
1099 26471–26487, doi:10.1029/97JC01283, 1997.

1100 Kendall, C. and Caldwell, E. A.: Fundamentals of Isotope Geochemistry, in *Isotope Tracers in
1101 Catchment Hydrology*, edited by C. Kendall and J. J. McDonnell, pp. 51–86, Elsevier,
1102 Amsterdam, Netherlands., 1998.

1103 Kirchner, J. W.: A double paradox in catchment hydrology and geochemistry, *Hydrol. Process.*,
1104 17(4), 871–874, doi:10.1002/hyp.5108, 2003.

1105 Klaus, J., McDonnell, J. J., Jackson, C. R., Du, E. and Griffiths, N. A.: Where does streamwater
1106 come from in low relief forested watersheds? A dual isotope approach, *Hydrol. Earth Syst.
1107 Sci.*, 19(1), 125–135, 2015.

1108 Koeniger, P., Leibundgut, C. and Stiehler, W.: Spatial and temporal characterisation of stable
1109 isotopes in river water as indicators of groundwater contribution and confirmation of modelling
1110 results; a study of the Weser river, Germany, *Isotopes Environ. Health Stud.*, 45(4), 289–302,
1111 doi:10.1080/10256010903356953, 2009.

1112 Kolaczyk, E. D.: *Statistical Analysis of Network Data with R*, Springer Science & Business
1113 Media, New York, NY, USA., 2014.

1114 Kortelainen, N. M. and Karhu, J. A.: Regional and seasonal trends in the oxygen and hydrogen
1115 isotope ratios of Finnish groundwaters: a key for mean annual precipitation, *J. Hydrol.*, 285(1–
1116 4), 143–157, doi:10.1016/j.jhydrol.2003.08.014, 2004.

1117 Kraft, P., Vaché, K. B., Frede, H. G. and Breuer, L.: CMF: A Hydrological Programming
1118 Language Extension For Integrated Catchment Models, *Environ. Model. Softw.*, 26(6), 828–
1119 830, doi:10.1016/j.envsoft.2010.12.009, 2011.

1120 Lai, C. T. and Ehleringer, J. R.: Deuterium excess reveals diurnal sources of water vapor in
1121 forest air, *Oecologia*, 165(1), 213–223, doi:10.1007/s00442-010-1721-2, 2011.

1122 Lauer, F., Frede, H. G. and Breuer, L.: Uncertainty assessment of quantifying spatially

1123 concentrated groundwater discharge to small streams by distributed temperature sensing, *Water*
1124 *Resour. Res.*, 49(1), 400–407, doi:10.1029/2012WR012537, 2013.

1125 LGR: Los Gatos Research, Greenhouse Gas, isotope and trace gas analyzers, [online] Available
1126 from: <http://www.lgrinc.com/> (Accessed 5 February 2013), 2013.

1127 Li, F., Song, X., Tang, C., Liu, C., Yu, J. and Zhang, W.: Tracing infiltration and recharge using
1128 stable isotope in Taihang Mt., North China, *Environ. Geol.*, 53(3), 687–696,
1129 doi:10.1007/s00254-007-0683-0, 2007.

1130 Maloszewski, P. and Zuber, A.: Manual on lumped parameter models used for the interpretation
1131 of environmental tracer data in groundwaters, in *Use of isotopes for analyses of flow and*
1132 *transport dynamics in groundwater systems*, p. 50, International Atomic Energy Agency,
1133 Vienna, Austria., 2002.

1134 McConville, C., Kalin, R. m., Johnston, H. and McNeill, G. w.: Evaluation of Recharge in a
1135 Small Temperate Catchment Using Natural and Applied $\delta^{18}\text{O}$ Profiles in the Unsaturated Zone,
1136 *Ground Water*, 39(4), 616–623, doi:10.1111/j.1745-6584.2001.tb02349.x, 2001.

1137 McDonnell, J. J. and Beven, K.: Debates—The future of hydrological sciences: A (common)
1138 path forward? A call to action aimed at understanding velocities, celerities and residence time
1139 distributions of the headwater hydrograph, *Water Resour. Res.*, 50(6), 5342–5350,
1140 doi:10.1002/2013WR015141, 2014.

1141 McDonnell, J. J., Sivapalan, M., Vaché, K., Dunn, S., Grant, G., Haggerty, R., Hinz, C., Hooper,
1142 R., Kirchner, J., Roderick, M. L. and others: Moving beyond heterogeneity and process
1143 complexity: a new vision for watershed hydrology, *Water Resour. Res.*, 43(7), W07301, 2007.

1144 McDonnell, J. J., McGuire, K., Aggarwal, P., Beven, K. J., Biondi, D., Destouni, G., Dunn, S.,
1145 James, A., Kirchner, J., Kraft, P., Lyon, S., Maloszewski, P., Newman, B., Pfister, L., Rinaldo,
1146 A., Rodhe, A., Sayama, T., Seibert, J., Solomon, K., Soulsby, C., Stewart, M., Tetzlaff, D.,
1147 Tobin, C., Troch, P., Weiler, M., Western, A., Worman, A. and Wrede, S.: How old is
1148 streamwater? Open questions in catchment transit time conceptualization, modelling and
1149 analysis, *Hydrol. Process.*, 24(12), 1745–1754, 2010.

1150 McGuire, K. J. and McDonnell, J. J.: A review and evaluation of catchment transit time
1151 modeling, *J. Hydrol.*, 330(3), 543–563, 2006.

1152 Michel, R. L.: Residence times in river basins as determined by analysis of long-term tritium
1153 records, *J. Hydrol.*, 130(1), 367–378, doi:10.1016/0022-1694(92)90117-E, 1992.

1154 Mook, W. G., Groeneveld, D. J., Brouwn, A. E. and Ganswijk, A. J. van: Analysis of a run-off
1155 hydrograph by means of natural ^{18}O , in *Isotope techniques in groundwater hydrology*, vol. 1,
1156 pp. 159–169, International Atomic Energy Agency, Vienna, Austria., 1974.

1157 Neal, C. and Rosier, P. T. W.: Chemical studies of chloride and stable oxygen isotopes in two
1158 conifer afforested and moorland sites in the British uplands, *J. Hydrol.*, 115(1–4), 269–283,
1159 doi:10.1016/0022-1694(90)90209-G, 1990.

1160 Newman, B., Tanweer, A. and Kurttas, T.: IAEA Standard Operating Procedure for the Liquid-
1161 Water Stable Isotope Analyser, *Laser Proceed. IAEA Water Resour. Programme*, 2009.

1162 O'Driscoll, M. A., DeWalle, D. R., McGuire, K. J. and Gburek, W. J.: Seasonal ^{18}O variations
1163 and groundwater recharge for three landscape types in central Pennsylvania, USA, *J. Hydrol.*,
1164 303(1–4), 108–124, doi:10.1016/j.jhydrol.2004.08.020, 2005.

1165 Orłowski, N., Frede, H. G., Brüggemann, N. and Breuer, L.: Validation and application of a

1166 cryogenic vacuum extraction system for soil and plant water extraction for isotope analysis, *J.*
1167 *Sens. Sens. Syst.*, 2(2), 179–193, doi:10.5194/jsss-2-179-2013, 2013.

1168 Orłowski, N., Lauer, F., Kraft, P., Frede, H. G. and Breuer, L.: Linking Spatial Patterns of
1169 Groundwater Table Dynamics and Streamflow Generation Processes in a Small Developed
1170 Catchment, *Water*, 6(10), 3085–3117, doi:10.3390/w6103085, 2014.

1171 Penna, D., Ahmad, M., Birks, S. J., Bouchaou, L., Brenčić, M., Butt, S., Holko, L., Jeelani, G.,
1172 Martínez, D. E., Melikadze, G., Shanley, J. B., Sokratov, S. A., Stadnyk, T., Sugimoto, A. and
1173 Vreča, P.: A new method of snowmelt sampling for water stable isotopes, *Hydrol. Process.*,
1174 28(22), 5637–5644, doi:10.1002/hyp.10273, 2014.

1175 Perry, C. and Taylor, K.: *Environmental Sedimentology*, p. 36, Blackwell Publishing, Oxford,
1176 OX, UK, 2009.

1177 Pierce, S. C., Kröger, R. and Pezeshki, R.: Managing Artificially Drained Low Gradient
1178 Agricultural Headwaters for Enhanced Ecosystem Functions, *Biology*, 1(3), 794–856,
1179 doi:10.3390/biology1030794, 2012.

1180 Qu, Y. and Duffy, C. J.: A semidiscrete finite volume formulation for multiprocess watershed
1181 simulation, *Water Resour. Res.*, 43(8), W08419, doi:10.1029/2006WR005752, 2007.

1182 Rinaldo, A., Benettin, P., Harman, C. J., Hrachowitz, M., McGuire, K. J., van der Velde, Y.,
1183 Bertuzzo, E. and Botter, G.: Storage selection functions: A coherent framework for quantifying
1184 how catchments store and release water and solutes, *Water Resour. Res.*, 51(6), 4840–4847,
1185 doi:10.1002/2015WR017273, 2015.

1186 Rohde, A.: Snowmelt Dominated Systems, in *Isotope Tracers in Catchment Hydrology*, edited
1187 by C. Kendall and J. J. McDonnell, pp. 391–433, Elsevier, Amsterdam, Netherlands., 1998.

1188 Rozanski, K., Sonntag, C. and Münnich, K. O.: Factors controlling stable isotope composition
1189 of European precipitation, *Tellus*, 34(2), 142–150, doi:10.1111/j.2153-3490.1982.tb01801.x,
1190 1982.

1191 Rozanski, K., Froehlich, K. and Mook, W. G.: in *Environmental isotopes in the hydrological
1192 cycle: Principles and Applications*, vol. 3, International Hydrological Programme; United
1193 Nations Educational, Scientific and Cultural Organization and International Atomic Energy
1194 Agency, Paris, Vienna., 2001.

1195 Schultz, N. M., Griffis, T. J., Lee, X. and Baker, J. M.: Identification and correction of spectral
1196 contamination in $^2\text{H}/^1\text{H}$ and $^{18}\text{O}/^{16}\text{O}$ measured in leaf, stem, and soil water, *Rapid Commun.*
1197 *Mass Spectrom.*, 25(21), 3360–3368, doi:10.1002/rem.5236, 2011.

1198 Shuttleworth, W. J. and Wallace, J. S.: Evaporation from sparse crops—an energy combination
1199 theory, *Q. J. R. Meteorol. Soc.*, 111(469), 839–855, doi:10.1002/qj.49711146910, 1985.

1200 Sklash, M. G.: Environmental isotope studies of storm and snowmelt runoff generation, in
1201 *Process studies in hillslope hydrology*, edited by M. G. Anderson, pp. 410–435, Wiley, New
1202 York, NY, USA., 1990.

1203 Sklash, M. G. and Farvolden, R. N.: The Role Of Groundwater In Storm Runoff, in
1204 *Developments in Water Science*, vol. 12, edited by W. B. and D. A. Stephenson, pp. 45–65,
1205 Elsevier, Amsterdam, Netherlands., 1979.

1206 Song, X., Wang, P., Yu, J., Liu, X., Liu, J. and Yuan, R.: Relationships between precipitation,
1207 soil water and groundwater at Chongling catchment with the typical vegetation cover in the
1208 Taihang mountainous region, China, *Environ. Earth Sci.*, 62(4), 787–796, doi:10.1007/s12665-

1209 010-0566-7, 2011.

1210 Stewart, M. K., Morgenstern, U. and McDonnell, J. J.: Truncation of stream residence time:
 1211 how the use of stable isotopes has skewed our concept of streamwater age and origin, *Hydrol.*
 1212 *Process.*, 24(12), 1646–1659, doi:10.1002/hyp.7576, 2010.

1213 Stumpp, C., Klaus, J. and Stichler, W.: Analysis of long-term stable isotopic composition in
 1214 German precipitation, *J. Hydrol.*, 517, 351–361, doi:10.1016/j.jhydrol.2014.05.034, 2014.

1215 Tang, K. and Feng, X.: The effect of soil hydrology on the oxygen and hydrogen isotopic
 1216 compositions of plants' source water, *Earth Planet. Sci. Lett.*, 185(3–4), 355–367, 2001.

1217 Taylor, S., Feng, X., Kirchner, J. W., Osterhuber, R., Klaue, B. and Renshaw, C. E.: Isotopic
 1218 evolution of a seasonal snowpack and its melt, *Water Resour. Res.*, 37(3), 759–769,
 1219 doi:10.1029/2000WR900341, 2001.

1220 Thomas, E. M., Lin, H., Duffy, C. J., Sullivan, P. L., Holmes, G. H., Brantley, S. L. and Jin, L.:
 1221 Spatiotemporal Patterns of Water Stable Isotope Compositions at the Shale Hills Critical Zone
 1222 Observatory: Linkages to Subsurface Hydrologic Processes, *Vadose Zone J.*, 12(4), 0,
 1223 doi:10.2136/vzj2013.01.0029, 2013.

1224 Timbe, E., Windhorst, D., Crespo, P., Frede, H. G., Feyen, J. and Breuer, L.: Understanding
 1225 uncertainties when inferring mean transit times of water trough tracer-based lumped-parameter
 1226 models in Andean tropical montane cloud forest catchments, *Hydrol. Earth Syst. Sci.*, 18(4),
 1227 1503–1523, doi:10.5194/hess-18-1503-2014, 2014.

1228 van der Velde, Y., Torfs, P. J. J. F., van der Zee, S. E. a. T. M. and Uijlenhoet, R.: Quantifying
 1229 catchment-scale mixing and its effect on time-varying travel time distributions, *Water Resour.*
 1230 *Res.*, 48(6), W06536, doi:10.1029/2011WR011310, 2012.

1231 Wang, X. F. and Yakir, D.: Using stable isotopes of water in evapotranspiration studies, *Hydrol.*
 1232 *Process.*, 14(8), 1407–1421, doi:10.1002/1099-1085(20000615)14:8<1407::AID-
 1233 HYP992>3.0.CO;2-K, 2000.

1234 Windhorst, D., Waltz, T., Timbe, E., Frede, H. G. and Breuer, L.: Impact of elevation and
 1235 weather patterns on the isotopic composition of precipitation in a tropical montane rainforest,
 1236 *Hydrol. Earth Syst. Sci.*, 17(1), 409–419, doi:10.5194/hess-17-409-2013, 2013.

1237 Windhorst, D., Kraft, P., Timbe, E., Frede, H. G. and Breuer, L.: Stable water isotope tracing
 1238 through hydrological models for disentangling runoff-generation processes at the hillslope
 1239 scale, *Hydrol. Earth Syst. Sci.*, 18(10), 4113–4127, doi:10.5194/hess-18-4113-2014, 2014.

1240 Woolfenden, L. R. and Ginn, T. R.: Modeled Ground-Water Age Distributions, *Ground Water*,
 1241 47(4), 547–557, doi:10.1111/j.1745-6584.2008.00550.x, 2009.

1242 Wu, J., Ding, Y., Ye, B., Yang, Q., Hou, D. and Xue, L.: Stable isotopes in precipitation in
 1243 Xilin River Basin, northern China and their implications, *Chin. Geogr. Sci.*, 22(5), 531–540,
 1244 doi:10.1007/s11769-012-0543-z, 2012.

1245 Xia, Y.: Optimization and uncertainty estimates of WMO regression models for the systematic
 1246 bias adjustment of NLDAS precipitation in the United States, *J. Geophys. Res. Atmospheres*,
 1247 111(D8), D08102, doi:10.1029/2005JD006188, 2006.

1248 Yurtsever, Y.: Worldwide survey of stable isotopes in precipitation, International Atomic
 1249 Energy Agency, Vienna, Austria., 1975.

1250 Zhao, L., Xiao, H., Zhou, J., Wang, L., Cheng, G., Zhou, M., Yin, L. and McCabe, M. F.:
 1251 Detailed assessment of isotope ratio infrared spectroscopy and isotope ratio mass spectrometry

1252 ~~for the stable isotope analysis of plant and soil waters, Rapid Commun. Mass Spectrom., 25(20),~~
1253 ~~3071–3082, doi:10.1002/rem.5204, 2011.~~
1254

1255 Table 1. Descriptive statistics of $\delta^2\text{H}$, $\delta^{18}\text{O}$, and d-excess values for precipitation, stream, and
 1256 groundwater over the two-year observation period including all sampling points.

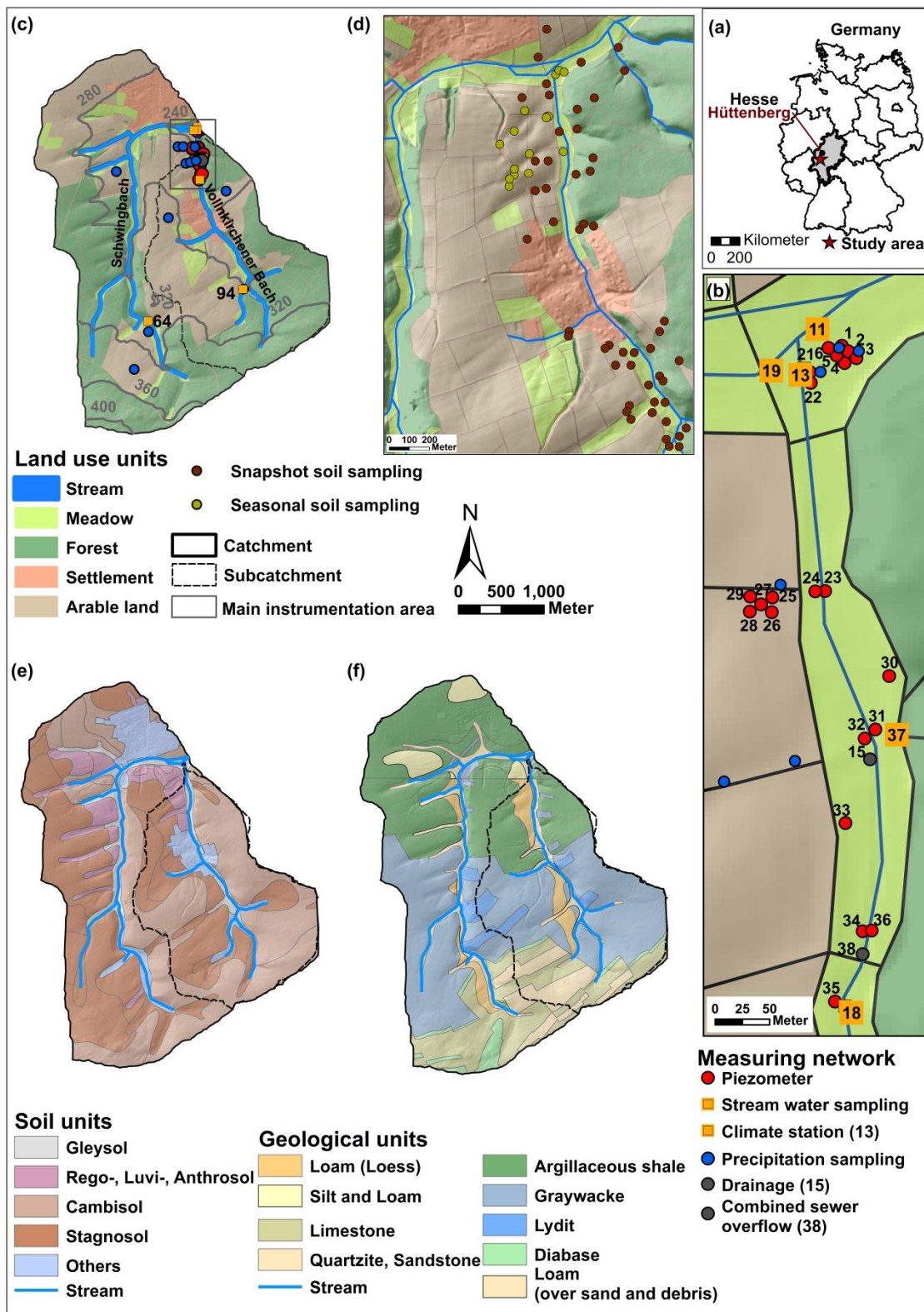
Sample type	Mean \pm SD		Min		Max		D-excess mean \pm SD	N
	$\delta^2\text{H}$	$\delta^{18}\text{O}$	$\delta^2\text{H}$	$\delta^{18}\text{O}$	$\delta^2\text{H}$	$\delta^{18}\text{O}$		
	[‰]	[‰]	[‰]	[‰]	[‰]	[‰]		
Precipitation	-43.9 \pm 23.4	-6.2 \pm 3.1	-167.6	-22.4	-8.3	-1.2	5.9 \pm 5.7	592
Vollnkirchener Bach	-58.0 \pm 2.8	-8.4 \pm 0.4	-66.3	-10.0	-26.9	-6.7	9.0 \pm 2.3	332
Schwingbach	-58.2 \pm 4.3	-8.4 \pm 0.6	-139.7	-18.3	-47.2	-5.9	9.0 \pm 2.2	463
Groundwater meadow	-57.6 \pm 1.6	-8.2 \pm 0.4	-64.9	-9.2	-50.8	-5.7	7.9 \pm 5.5	375
Groundwater arable land	-56.2 \pm 3.7	-8.0 \pm 0.5	-91.6	-12.3	-49.5	-6.8	1.7 \pm 5.0	338
Groundwater along stream	-59.9 \pm 6.8	-8.5 \pm 0.9	-94.5	-13.0	-49.5	-7.0	8.2 \pm 1.5	108

1257

1258 Table 2. Mean and standard deviation (SD) for isotopic signatures and soil physical properties in 0.2 m and 0.5 m soil depth (N=52 per depth).

	$\delta^2\text{H}$ [‰]		$\delta^{18}\text{O}$ [‰]		water content [% w/w]		pH		bulk density [g cm ⁻³]	
	0.2 m	0.5 m	0.2 m	0.5 m	0.2 m	0.5 m	0.2 m	0.5 m	0.2 m	0.5 m
Mean±SD	-46.9±8.4	-58.5±8.3	-6.6±1.2	-8.2±1.2	16.8±7.2	16.1±8.3	5.0±1.0	5.3±1.0	1.3±0.2	1.3±0.2

1259



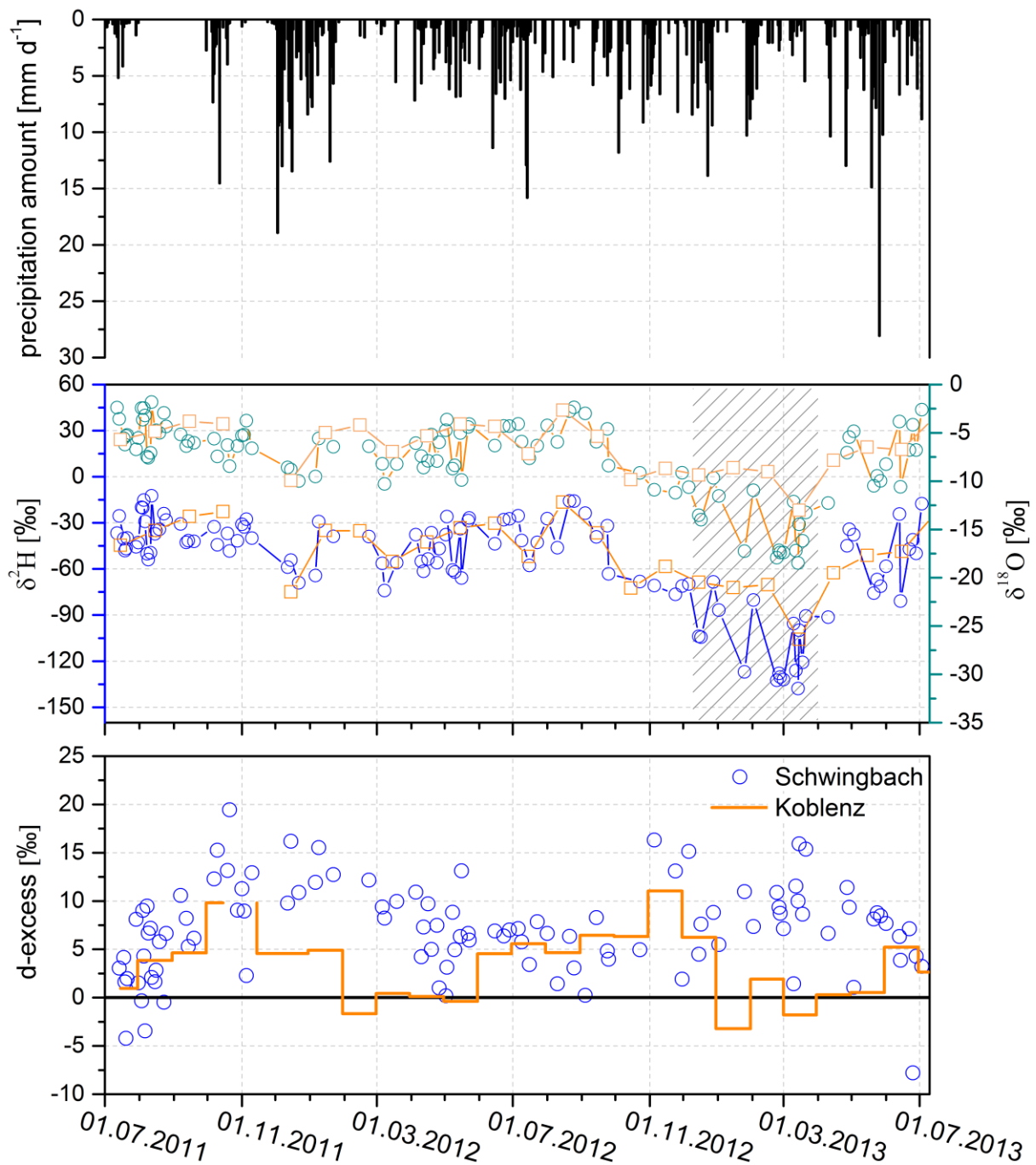
1260

1261

1262 Figure 1. Maps show (a) the location of the Schwingbach catchment in Germany, (b) the main

1263 main monitoring area, (c) the land use, elevation, and instrumentation, (d) the locations of the

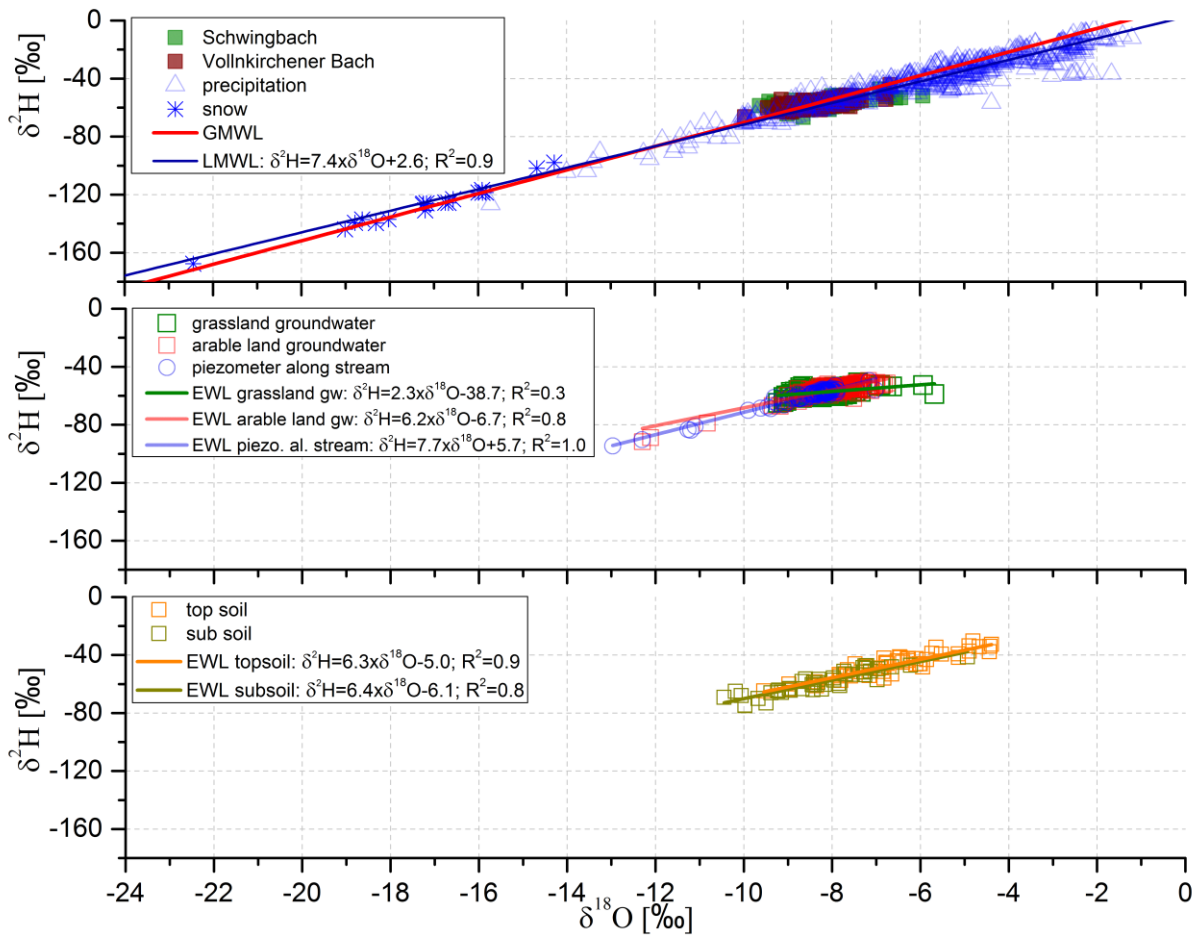
1264 snapshot as well as the seasonal soil samplings, (e) soil types, and (f) geology of the
1265 Schwingbach catchment including the Vollnkirchener Bach subcatchment boudaries.
1266



1267
1268

1269 Figure 2. Temporal variation of precipitation amount, isotopic signatures ($\delta^2\text{H}$ and $\delta^{18}\text{O}$)
 1270 including snow samples (grey striped box) of the Schwingbach and GNIP station Koblenz, and
 1271 d-excess values for the study area compared to monthly d-excess values (July 2011 to July
 1272 2013) of GNIP station Koblenz with reference d-excess of GMWL ($d=10$; solid black line).

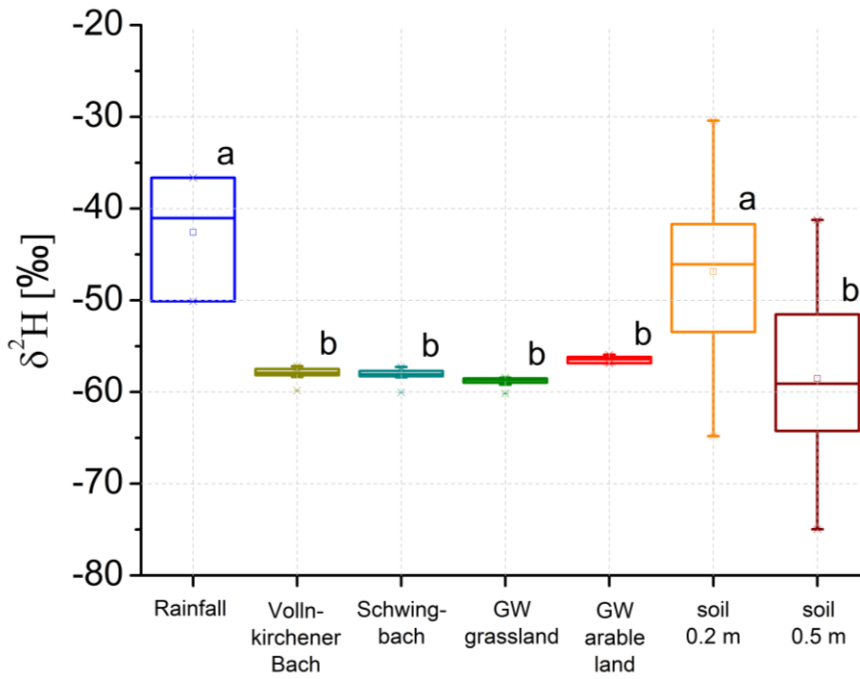
1273



1274

1275

1276 Figure 3. Local Meteoric Water Line for the Schwingbach catchment (LMWL) in comparison
 1277 to GMWL, including comparisons between precipitation, stream water, groundwater, and soil
 1278 water isotopic signatures and the respective EWLs.

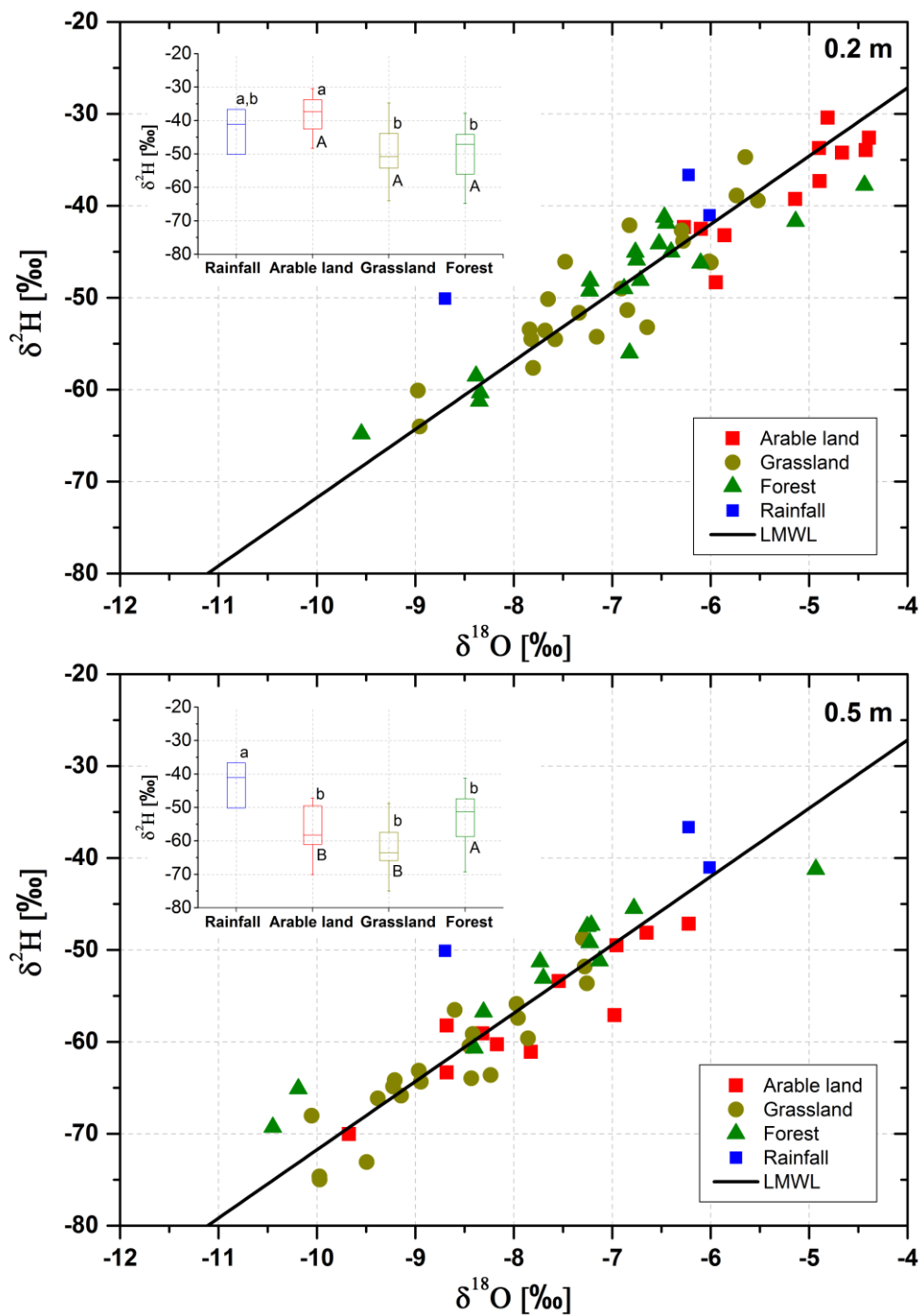


1279

1280

1281 Figure 4. Boxplots of $\delta^2\text{H}$ values comparing precipitation, stream, groundwater, and soil
 1282 isotopic composition in 0.2 m and 0.5 m depth (N=52 per depth). Different letters indicate
 1283 significant differences ($p \leq 0.05$).

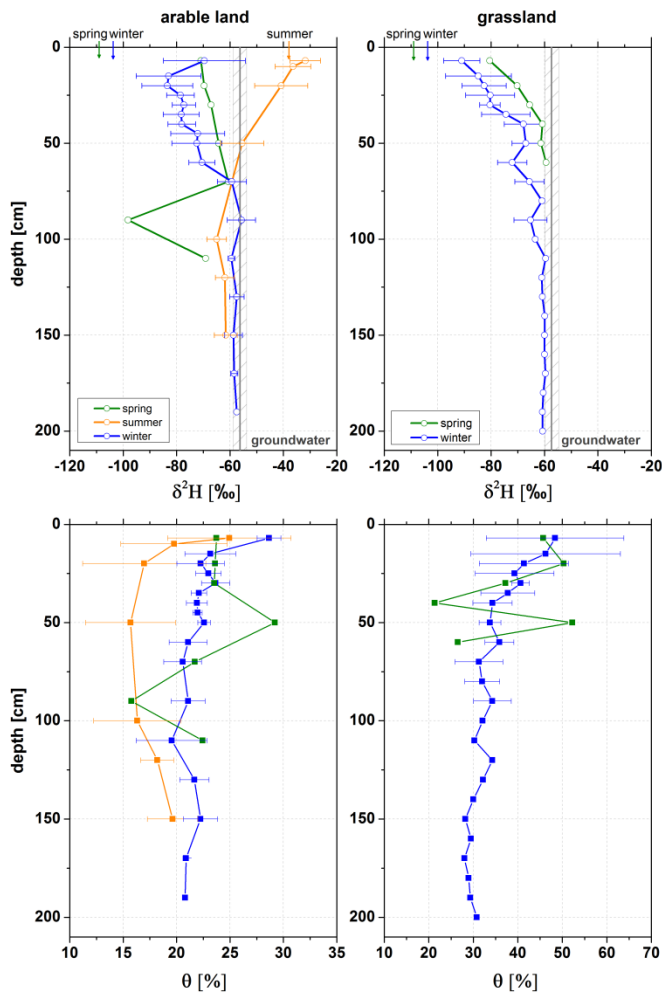
1284



1285

1286

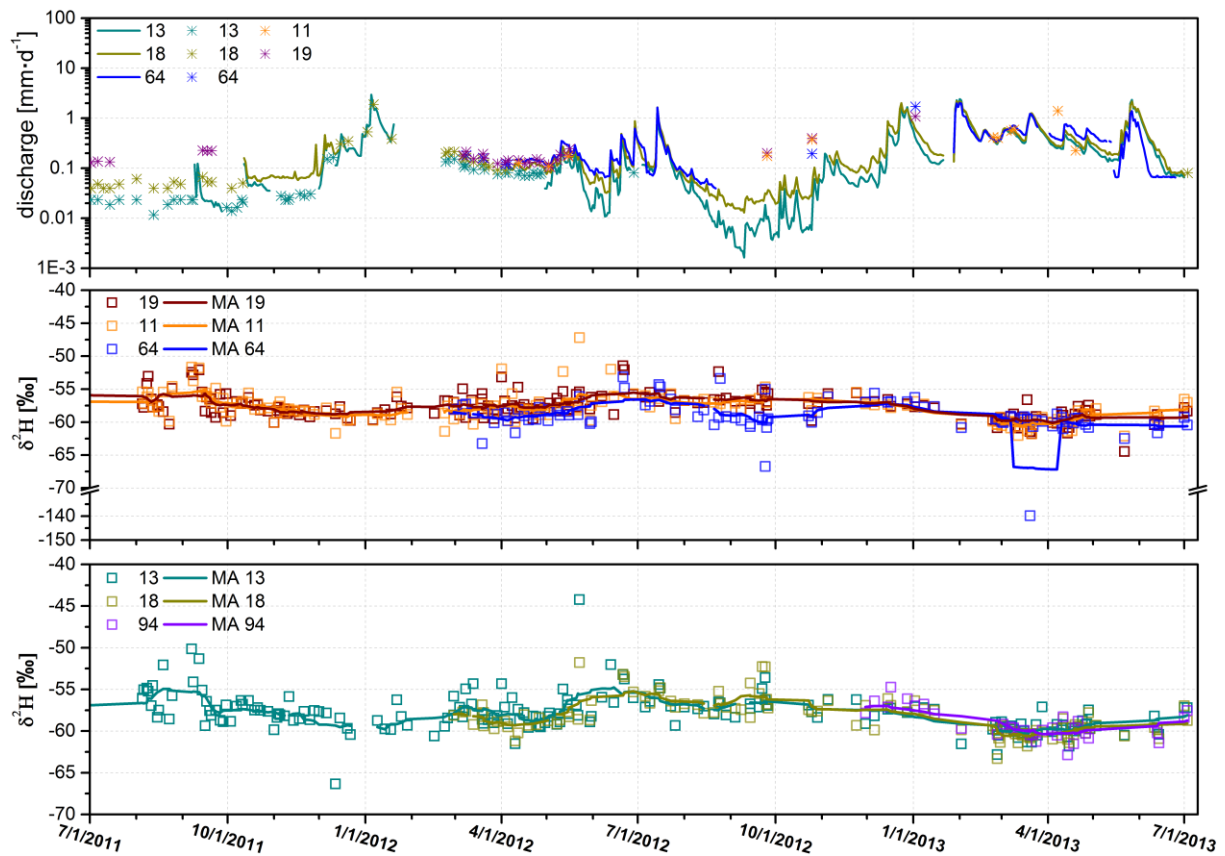
1287 Figure 5. Dual isotope plot of soil water isotopic signatures in 0.2 m and 0.5 m depth compared
 1288 by land use including precipitation isotope data from 19, 21, and 28 October 2011. Insets:
 1289 Boxplots comparing $\delta^2\text{H}$ isotopic signatures between different land use units and precipitation
 1290 (small letters) in top and subsoil (capital letters). Different letters indicate significant
 1291 differences ($p \leq 0.05$).



1292

1293

1294 Figure 6. Seasonal $\delta^2\text{H}$ profiles of soil water (upper panels) and water content (lower panels)
 1295 for winter (28 March 2013), summer (28 August 2011), and spring (24 April 2013). Error bars
 1296 represent the natural isotopic variation of the replicates taken during each sampling campaign.
 1297 For reference, mean groundwater (grey shaded) and mean seasonal precipitation $\delta^2\text{H}$ values are
 1298 shown (coloured arrows at the top).



1299

1300

1301 Figure 7. Mean daily discharge at the Vollnkirchener Bach (13, 18) and Schwingbach (site 11,

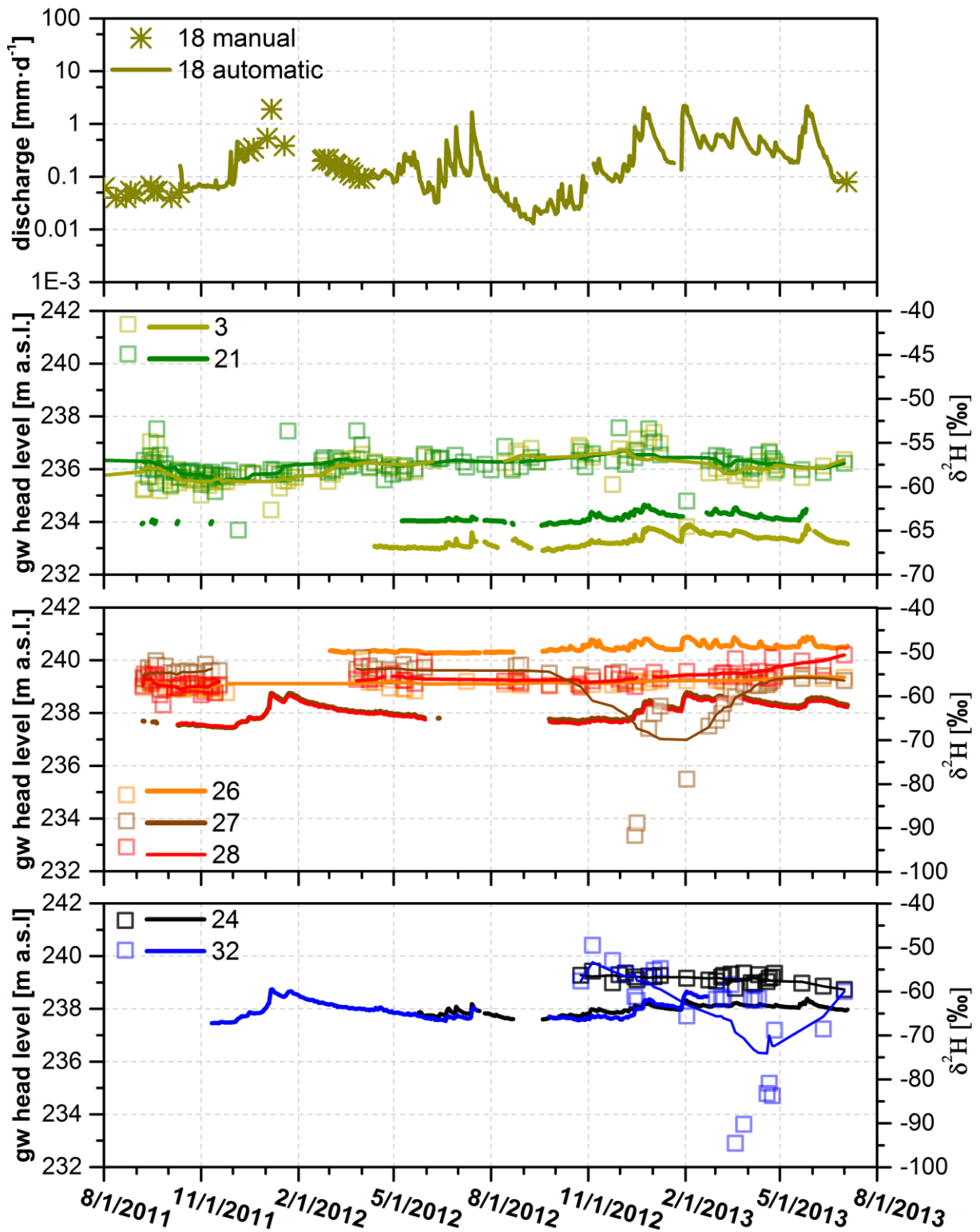
1302 19, and 64) with automatically recorded data (solid lines) and manual discharge measurements

1303 (asterisks), temporal variation of $\delta^2\text{H}$ of stream water in the Schwingbach (site 11, 19, and 64)

1304 and Vollnkirchener Bach (site 13, 18, and 94) including moving averages (MA) for streamflow

1305 isotopes.

1306

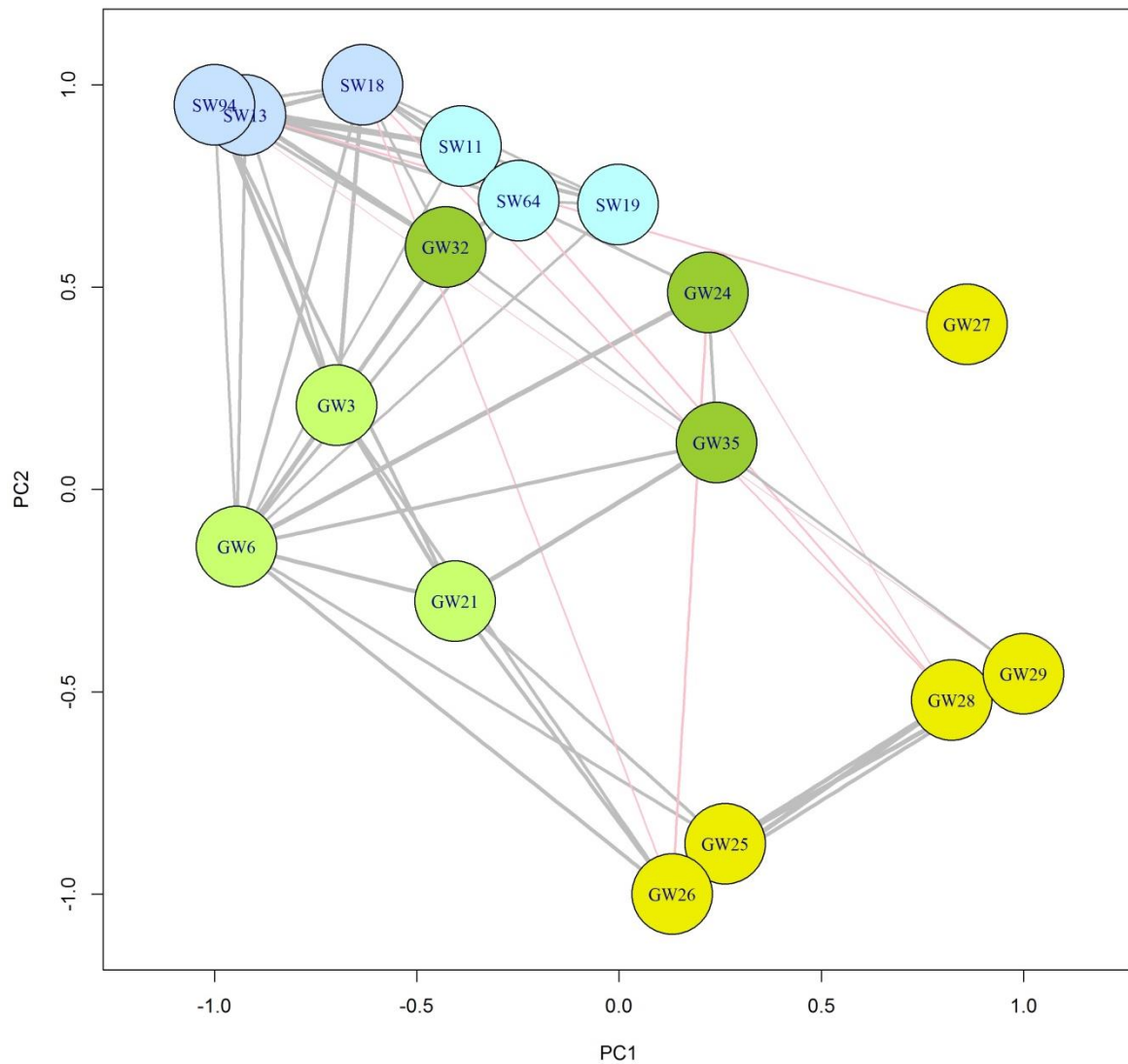


1307

1308

1309 Figure 8. Temporal variation of discharge at the Vollnkirchener Bach with automatically
 1310 recorded data (solid line) and manual discharge measurements (asterisks) (site 18), groundwater
 1311 head levels, and $\delta^2\text{H}$ values (coloured dots) for selected piezometers under meadow (site 3 and

1312 21), arable land (site 26, 27, and 28), and beside the Vollnkirchener Bach (site 24 and 32)
1313 including moving averages for groundwater isotopes.

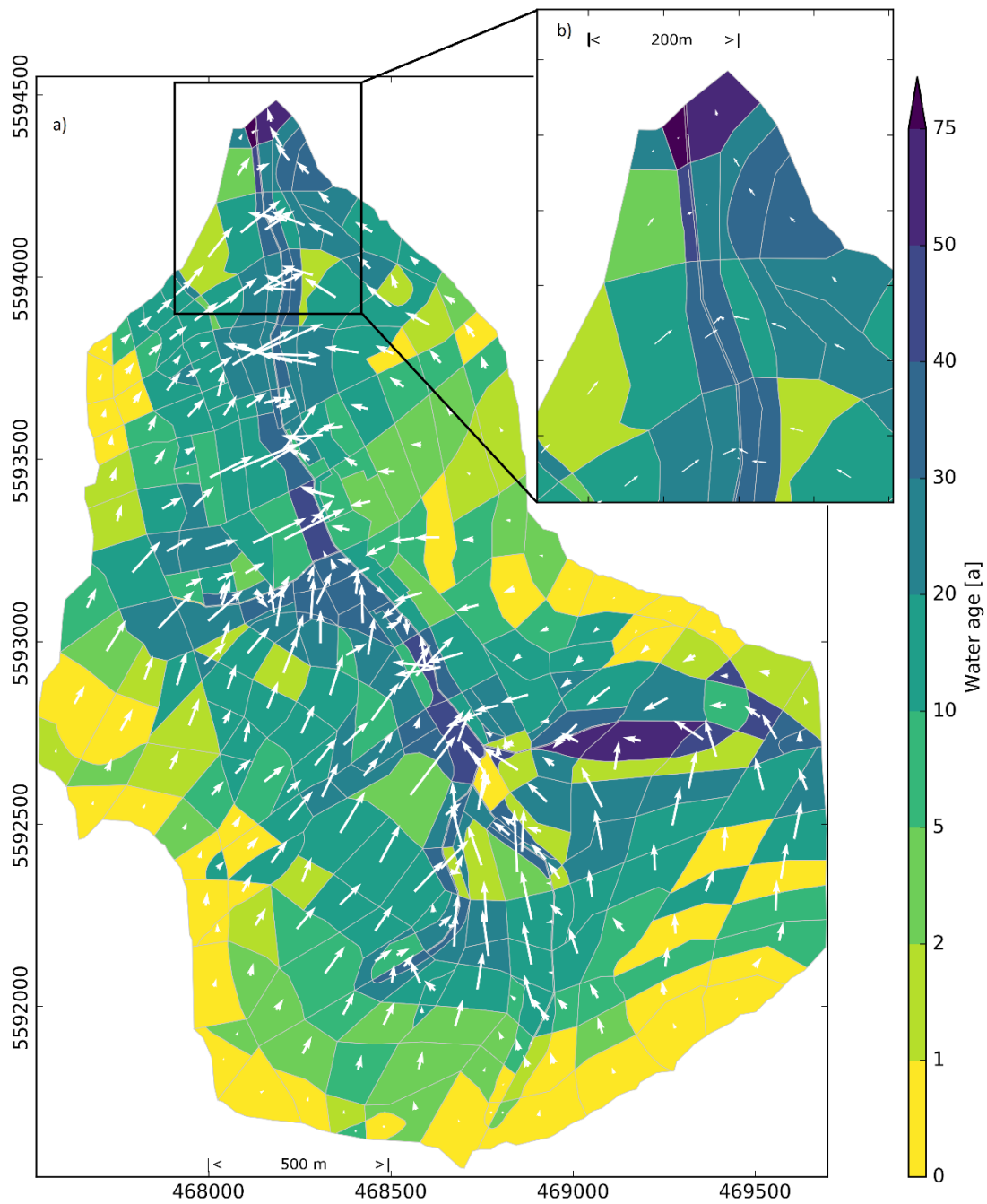


1314

1315

1316 Figure 9. Network map of $\delta^{18}\text{O}$ relationships between surface water (SW) and groundwater
 1317 (GW) sampling points. Yellow circles represent groundwater sampling points on the arable
 1318 field, light green circles are piezometers located on the grassland close to the conjunction of the
 1319 Schwingbach with the Vollnkirchener Bach, and dark green circles represent piezometers along
 1320 the Vollnkirchener Bach. Light blue circles stand for Schwingbach and darker blue circles for
 1321 Vollnkirchener Bach surface water sampling points. See Figure 1 for an overview of all
 1322 sampling points. Only statistically significant connections between $\delta^{18}\text{O}$ time series ($p < 0.05$)
 1323 are shown in the network diagram.

1324



1325

1326

1327 Figure 10. Maps of modelled groundwater ages (colour scheme) and flow directions (white
 1328 arrows) of (a) the Vollnkirchner Bach subcatchment and (b) detail view of the northern part of
 1329 the subcatchment. The length of the white arrows depicts the intensity of flow. UTM-32N
 1330 (WGS84) coordinates on the axis. The intensity of flow is depicted by the length of the white
 1331 arrows.

1332

1333 **Appendix I**

1334 **Mean transit time estimation**

1335 We applied a set of five different models to estimate the MTT using the FlowPC software
1336 (Maloszewski and Zuber, 2002): dispersion model (with different dispersion parameters
1337 $D_p=0.05, 0.4, \text{ and } 0.8$), exponential model, exponential-piston-flow model, linear model, and
1338 linear-piston-flow model. We evaluated these results using two goodness of fit criteria, i.e.
1339 sigma (σ) and model efficiency (ME) following Maloszewski and Zuber (2002):

$$\sigma = \frac{\sqrt{\sum (c_{mi} - c_{oi})^2}}{m} \quad (1)$$

$$ME = 1 - \frac{\sum (c_{mi} - c_{oi})^2}{\sum (c_{oi} - \bar{c}_o)^2} \quad (2)$$

1340 Where:

- 1341 • c_{mi} : The i-th model result
- 1342 • c_{oi} : The i-th observed result
- 1343 • \bar{c}_o : The arithmetic mean of all observations

1344

1345 A model efficiency $ME=1$ indicates an ideal fit of the model to the concentrations observed,
1346 while $ME=0$ indicates that the model fits the data no better than a horizontal line through the
1347 mean observed concentration (Maloszewski and Zuber, 2002). The same is true for sigma. For
1348 calculations with FlowPC, weekly averages of precipitation and stream water isotopic
1349 signatures are calculated. We firstly calculated the MTT from precipitation to the streams for
1350 three sampling points in the Vollnkirchener Bach (sites 13, 18 and 94) and three points in the
1351 Schwingbach (sites 11, 19 and 64). For the second set of simulations, the mean residence time
1352 from precipitation to groundwater comprising thirteen groundwater sampling points was
1353 determined. We also bias-corrected the precipitation input data with two different approaches:
1354 the mean precipitation value is subtracted from every single precipitation value and then divided
1355 by the standard deviation of precipitation isotopic signatures. Afterwards, this value is
1356 subtracted from the weekly precipitation values (bias1). For the second approach, the difference
1357 of the mean stream water isotopic value and the mean precipitation value is calculated and also
1358 subtracted from the weekly precipitation values (bias2).

1359

1360 **Appendix II**

1361 **Model-based groundwater age dynamics**

1362 Objective:

1363 Stable water isotopes are only a tool to determine the residence time for a few years (McDonnell
1364 et al., 2010). In cases of longer residence times and a strong mixing effect, seasonal variation
1365 of isotopes vanishes and results in barely varying isotopic signals. To get a rough estimate of
1366 residence times greater than the limit of stable water isotopes (>5 years), we split the water flow
1367 path in our catchment in two parts: the flow from precipitation to groundwater, which was
1368 calculated via FlowPC and the longer groundwater transport. The simplest method to estimate
1369 the residence time of groundwater transport is via the storage-to-input-relation, with the storage
1370 as the aquifer size and the input as the groundwater recharge time. However, this method
1371 ignores the topographic setting, and water input heterogeneity. In our study we used a simplified
1372 groundwater flow model with tracer transport to calculate the groundwater age dynamics. The
1373 numerical output of water ages cannot be validated with the given isotope data, since the model
1374 is used to fill a residence time gap, where stable water isotopes are not feasible to apply. The
1375 model is falsified however, if the residence time is short enough (<5 years) to be calculable via
1376 FlowPC. Hence, the results of the groundwater age model should be handled with care and only
1377 seen as the order of magnitude of flow time scales.

1378 Model setup:

1379 We set up a tailored hydrological model for the Vollnkirchener Bach subcatchment using the
1380 *Catchment Modelling Framework* (CMF) by Kraft et al. (2011). CMF is a modular framework
1381 for hydrological modelling based on the concept of finite volume method by Qu and Duffy
1382 (2007). CMF is applicable for simulating one- to three-dimensional water fluxes but also
1383 advective transport of stable water isotopes (^{18}O and ^2H). Thus, it is especially suitable for our
1384 tracer study and can be used to study the origin (Windhorst et al., 2014) and age of water. To
1385 avoid errors in transit time calculations from small differences between the isotopic signal in
1386 groundwater and stream water, we are tracing the transit time of groundwater and not the real
1387 isotopic values in this study. The generated model is a highly simplified representation of the
1388 Vollnkirchener Bach subcatchment's groundwater body. The subcatchment is divided into 353
1389 polygonal-shaped cells ranging from 100–40'000 m² in size based on land use, soil type, and
1390 topography. The model is vertically divided in two compartments, the upper soft rock aquifer,
1391 and the lower bed rock aquifer, referred to as upper and lower layer from now onwards.

1392 The layers of each cell are connected using a mass conservative Darcy approach with a finite
 1393 volume discretization. The water storage dynamic of one layer in one cell i of the groundwater
 1394 model is given as:

$$\frac{dV_{i,s}}{dt} = R_i - S_i - \sum_{j=1}^{N_i} \left(K_s \frac{\Psi_{i,s} - \Psi_{j,s}}{d_{ij}} A_{ij,s} \right) \quad (3)$$

$$\frac{dV_{i,b}}{dt} = S_i - \sum_{j=1}^{N_i} \left(K_b \frac{\Psi_{i,b} - \Psi_{j,b}}{d_{ij}} A_{ij,b} \right)$$

1395

1396 Where:

- 1397 • V_i : The water volume stored by the layer in m^3 in cell I for soft rock (s) and bedrock
 1398 (b), respectively
- 1399 • R_i : The groundwater recharge rate in $\text{m}^3 \cdot \text{d}^{-1}$
- 1400 • S_i : the percolation from the soft rock to the bedrock aquifer, calculated by the
 1401 gradient and geometric mean conductivity between the layers: $S_i =$
 1402 $\sqrt{K_s K_b} \frac{\Psi_{i,s} - \Psi_{i,b}}{d_{sb}} A_i$, where d_{sb} is the distance between the layers and A_i is the cell area
- 1403 • N_i : Number of adjacent cells to cell i
- 1404 • K : Saturated hydraulic conductivity in $\text{m} \cdot \text{d}^{-1}$ for soft rock (s) and bedrock (b),
 1405 respectively
- 1406 • Ψ : Water head in the current cell i and the neighbour cell j in m for soft rock (s) and
 1407 bedrock (b), respectively
- 1408 • d_{ij} : The distance between the current cell i and the neighbour cell j in m
- 1409 • $A_{i,j,x}$: The wetted area of the joint layer boundary in m^2 between cells i and j in layer
 1410 x

1411 The volume head relation is linearized as $\Psi = \phi \frac{V}{A}$, with ϕ being the fillable porosity and A the
 1412 cell area. The resulting ordinary differential equation system is integrated using the CVODE
 1413 solver by Hindmarsh et al. (2005), an error controlled Krylov-Newton multistep implicit solver
 1414 with an adaptive order of 1–5 according to stability constraints.

1415 Boundary conditions:

1416 The upper boundary condition of the groundwater system – the mean groundwater recharge –
1417 is modelled applying a Richard's equation based model using measured rainfall data (2011–
1418 2013) and calculated evapotranspiration with the Shuttleworth-Wallace method (Shuttleworth
1419 and Wallace, 1985) including land cover and climate data. To retrieve long-term steady state
1420 conditions, the groundwater recharge is averaged and used as constant flow Neumann boundary
1421 condition. The total outflow is calibrated against measured outflow data; hence, the unsaturated
1422 model's role is mainly to account for spatial heterogeneity of groundwater recharge. As an
1423 additional input, a combined sewer overflow (site 38, Fig. 1b) is considered based on findings
1424 of Orłowski et al. (2014). Moreover, there are two water outlets in the two lowest cells for
1425 efficient draining, reflecting measured groundwater flow directions throughout most of the year
1426 at piezometers 1–6 (Fig. 1b). Both cells are located in the very north of the subcatchment and
1427 their outlets are modelled as constant head Dirichlet boundary condition.

1428 Parameters:

1429 The saturated hydraulic conductivity of the groundwater body is set to 0.1007 m d^{-1} , as
1430 measured in the study area. For the lower bedrock compartment there is no data available.
1431 However, expecting a high rate of joints, preliminary testing revealed that a saturated hydraulic
1432 conductivity of 0.25 m d^{-1} seemed to be a realistic estimation (based on field measurements).

1433 Water Age:

1434 To calculate the water age in each cell, a virtual tracer flows through the system using advective
1435 transport. To calculate the water age from the tracer that enters the system with a unity
1436 concentration by groundwater recharge, a linear decay is used to reduce the tracer concentration
1437 with time:

$$\frac{dX_{i,s}}{dt} = 1 \frac{u}{m^3} R_i - S_i [X]_{i,s} - \sum_{j=1}^{N_i} \left([X]_{i,s} K_s \frac{\Psi_{i,s} - \Psi_{j,s}}{d_{ij}} A_{ij,s} \right) - r X_{i,s} \quad (4)$$
$$\frac{dX_{i,b}}{dt} = S_i [X]_{i,s} - \sum_{j=1}^{N_i} \left([X]_{i,b} K_b \frac{\Psi_{i,b} - \Psi_{j,b}}{d_{ij}} A_{ij,b} \right) - r X_{i,b}$$

$$t_{ix} = \frac{\ln[X]_{ix}}{r}$$

1438

1439 Where:

- 1440 • $X_{i,x}$: Amount of virtual tracer in layer x in cell i in virtual unit u
- 1441 • $1 \frac{u}{m^3} R_i$: Tracer input with groundwater recharge R with unity concentration
- 1442 • $[X]_{i,x}$: Concentration of tracer in layer x of cell i in $u m^{-3}$
- 1443 • r : Arbitrary chosen decay constant, for water age calculation in d^{-1} . Rounding errors
- 1444 occur due to low concentrations when r is set to a high value. We found a good
- 1445 numerical performance with values between 10^{-6} – $10^{-9} d^{-1}$
- 1446 • t_{ix} : Water age in days in layer x in cell i

1447

1448 To ensure long term steady state conditions, the model is run for 2000 years. However, after
1449 300 years of model run time, steady state is reached.